การพัฒนาสมรรถนะของระบบเซลล์เชื้อเพลิงชนิดออกไซด์แข็งที่ป้อนด้วยเอทานอลชีวภาพด้วยเพอร์แวปพอเรชัน

นายวรฉัตร สุขวัฒนจรูญ

วิทยานิพนธ์นี้เป็นส่วนหนึ่งของการศึกษาตามหลักสูตรปริญญาวิศวกรรมศาสตรมหาบัณฑิต
สาขาวิชาวิศวกรรมเคมี ภาควิชาวิศวกรรมเคมี
คณะวิศวกรรมศาสตร์ จุฬาลงกรณ์มหาวิทยาลัย
ปีการศึกษา 2553

PERFORMANCE IMPROVEMENT OF BIOETHANOL-FUELLED SOLID OXIDE FUEL CELL SYSTEM WITH PERVAPORATION

Mr. Vorachatra Sukwattanajaroon

A Thesis Submitted in Partial Fulfillment of the Requirements
for the Degree of Master of Engineering Program in Chemical Engineering
Department of Chemical Engineering
Faculty of Engineering
Chulalongkorn University
Academic Year 2010

Thesis Title	PERFORMANCE IMPROVEMENT OF BIOETHANOL-FUELLED SOLID OXIDE FUEL CELL SYSTEM WITH PERVAPORATION
By	Mr. Vorachatra Sukwattanajaroon
Field of Study	Chemical Engineering
Thesis Advisor	Professor Suttichai Assabumrungrat, Ph.D.
Thesis Co-advisor	Sumittra Charojrochkul, Ph.D.

Accepted by the Faculty of Engineering, Chulalongkorn University in Partial Fulfillment of the Requirements for the Master's Degree

..... Dean of the Faculty of Engineering

(Associate Professor Boonsom Lerdhirunwong, Dr.Ing.)

THESIS COMMITTEE

..... Chairman

(Assistant Professor Anongnat Somwangthanaroj, Ph.D.)

..... Thesis Advisor

(Professor Suttichai Assabumrungrat, Ph.D.)

..... Thesis Co-advisor

(Sumittra Charojrochkul, Ph.D.)

Bunjerd Jongsomjit ..... Examiner

(Associate Professor Bunjerd Jongsomjit, Ph.D.)

..... External Examiner

(Assistant Professor Worapon Kiatkittipong, D.Eng.)

วรฉัตร สุขวัฒนจรูญ : การพัฒนาสมรรถนะของระบบเซลล์เชื้อเพลิงชนิดออกไซด์แข็งที่ป้อนด้วยเอทานอลชีวภาพด้วยเพอร์แวปพอเรชัน. (PERFORMANCE IMPROVEMENT OF BIOETHANOL-FUELLED SOLID OXIDE FUEL CELL SYSTEM WITH PERVAPORATION) อ. ที่ปรึกษาวิทยานิพนธ์หลัก: ศ.ดร.สุทธิชัย อัสสะบำรุงรัตน์, อ. ที่ปรึกษาวิทยานิพนธ์ร่วม: ดร.สุมิตรา จรสโรจน์กุล, 74 หน้า.

งานวิจัยนี้ศึกษาการพัฒนาสมรรถนะของระบบเซลล์เชื้อเพลิงชนิดออกไซด์แข็งที่ป้อนเชื้อเพลิงด้วยเอทานอลชีวภาพด้วยเพอร์แวปพอเรชัน เมมเบรนสองชนิดซึ่งได้แก่ ชนิดชอบน้ำและชนิดไม่ชอบน้ำได้ถูกนำมาใช้ในเพอร์แวปพอเรชันซึ่งถูกรวมเข้ากับระบบเซลล์เชื้อเพลิงชนิดออกไซด์แข็งเพื่อนำมาทดสอบเปรียบเทียบประสิทธิภาพทางไฟฟ้า จากการศึกษาระบุว่าเพอร์แวปพอเรชันที่ใช้เมมเบรนชนิดไม่ชอบน้ำต้องการพลังงานความร้อนน้อยกว่าประมาณหนึ่งในสี่ของกรณีเพอร์แวปพอเรชันที่ใช้เมมเบรนชนิดชอบน้ำส่งผลให้ระบบที่ใช้เมมเบรนชนิดไม่ชอบน้ำให้ประสิทธิภาพทางไฟฟ้าโดยรวมที่สูงกว่าระบบที่ใช้เมมเบรนชนิดชอบน้ำ เนื่องจากเมมเบรนชนิดไม่ชอบน้ำต้องการค่าตัวแปรการแยก (separation factor) ที่สูงเมื่อเพอร์แวปพอเรชันถูกดำเนินงานที่ค่าการนำกลับเอทานอลที่สูงเพื่อให้ได้รับประสิทธิภาพทางไฟฟ้าที่สูงขึ้น อย่างไรก็ตามในความเป็นจริงเมมเบรนชนิดไม่ชอบน้ำมีค่าตัวแปรการแยกที่ต่ำ ดังนั้นต่อมาเวเปอร์เพอร์มิเอชันจึงถูกนำเสนอให้ติดตั้งเพิ่มเติมต่อจากเพอร์แวปพอเรชันเพื่อแก้ปัญหาดังที่กล่าวมา การทดลอง ณ สภาวะที่ระบบสามารถพึ่งพาพลังงานในระบบเองได้ และใช้เมมเบรน PTMSP ซึ่งมีสมรรถนะการแยกที่ต่ำที่สุดเทียบกับเมมเบรนที่นำมาทดลองทั้งหมด ผลที่ได้จากแบบจำลองพบว่าระบบที่ติดตั้งเวเปอร์เพอร์มิเอชันชนิดชอบน้ำเพิ่มเข้าไปสามารถให้ประสิทธิภาพทางไฟฟ้าประมาณ 2.4 เท่าเมื่อเทียบกับกรณีติดตั้งเฉพาะเพอร์แวปพอเรชัน สำหรับการเปรียบเทียบสมรรถนะของระบบโดยรวมเมื่อใช้กระบวนการทำเอทานอลชีวภาพให้บริสุทธิ์ชนิดต่างๆ พบว่าสามารถเรียงลำดับกระบวนการที่ให้ประสิทธิภาพทางไฟฟ้าโดยรวมจากสูงไปต่ำได้ดังนี้ ระบบร่วมเวเปอร์เพอร์มิเอชันและเพอร์แวปพอเรชัน > เพอร์แวปพอเรชัน > หอกลั่น ตามลำดับ

ภาควิชา วิศวกรรมเคมี ลายมือชื่อนิสิต Vorachatt Sukwattanajaroon

สาขาวิชา วิศวกรรมเคมี ลายมือชื่อ อ.ที่ปรึกษาวิทยานิพนธ์หลัก

ปีการศึกษา 2553 ลายมือชื่อ อ.ที่ปรึกษาวิทยานิพนธ์ร่วม

#5270474921 : MAJOR CHEMICAL ENGINEERING

KEYWORDS : SOLID OXIDE FUEL CELL (SOFC)/ BIOETHANOL / SIMULATION

VORACHATRA SUKWATTANAJAROON: PERFORMANCE IMPROVEMENT OF BIOETHANOL-FUELLED SOLID OXIDE FUEL CELL SYSTEM WITH PERVAPORATION. ADVISOR: PROF. SUTTICHAI ASSABUMRUNGRAT, Ph.D., CO-ADVISOR: SUMITTRA CHAROJROCHKUL, Ph.D., 74 pp.

This research investigated the performance improvement of bioethanol-fuelled Solid Oxide Fuel Cell (SOFC) system with pervaporation. Two types of membrane, hydrophilic and hydrophobic were employed in a pervaporation integrated with SOFC system and their corresponding overall electrical efficiencies were compared. The results indicated that the system with hydrophobic membrane required much less thermal energy about 1/4 times and offered a higher overall electrical efficiency compared to the system with hydrophilic membrane. High ethanol separation factor values of hydrophobic membrane were required when the purification system was operated at higher ethanol recovery to achieve more overall efficiency. However, the real membranes which had high enough separation factor values of the hydrophobic type were limited. Afterwards, vapor permeation was proposed to be further installed after a hydrophobic pervaporation (hybrid vapor permeation-pervaporation) to solve the previous problem. Based on energy self-sufficient condition and PTMSP membrane regarded as the poorest separation performance, the simulation results showed that it could offer the overall electrical efficiency of about 2.4 times when installing a hydrophilic vapor permeation compared with the case of using the pervaporation alone. Among the different purification processes at base case, the overall electrical efficiency can be ranked by the following order: Hybrid vapor permeation-pervaporation > pervaporation > distillation column, respectively.

Department : Chemical Engineering	Student's Signature Vorachatra Sukwattanajaroon
Field of Study : Chemical Engineering	Advisor's Signature
Academic Year : 2010	Co-advisor's Signature

ACKNOWLEDGEMENTS

The author would like to express high gratitude and appreciation to his advisor, Professor Suttichai Assabumrungrat, for his useful guidance, cultivating problem solving skill and good willpower throughout the author's research study period and his co-advisor, Dr. Sumittra Charojrochkul, a researcher at National Metal and Materials Technology Center (MTEC), Thailand, for her valuable suggestions and useful knowledge in Solid Oxide Fuel Cell. Special thank to Assistant Professor Anongnat Somwangthanaroj as the chairman, Associate Professor Bunjerd Jongsomjit and Assistant Professor Worapon Kiatkittipong as the members of the thesis committee.

Sincere thanks to National Science and Technology Development Agency (NSTDA), Thailand, and Faculty of Engineering, Chulalongkorn University, for providing scholarships to support this research and his Master's Degree study.

The author wishes to thank all members in Center of Excellence on Catalysis and Catalytic Reaction Engineering, Department of Chemical Engineering, Faculty of Engineering, Chulalongkorn University for a good memory and warm friendship during the period of his study.

Finally, it would not be here without his beloved parents and grandmother, who have given him great encouragements when he faced obstacles in his study. The virtues of this work are dedicated to them.

CONTENTS

CHAPTERS Page

CHAPTERS Page

LIST OF TABLES

LIST OF FIGURES

Figure Page

NOMENCLATURES

A	cell stack area	[m^2]
C_P	heat capacity	[J mol^{-1} K^{-1}]
$D_{i,K}$	Knudsen diffusivity of component *i*	[cm^2 s^{-1}]
D_{A-B}	ordinary diffusivity of gas A versus gas B	[cm^2 s^{-1}]
$D_{i\ (eff)}$	effective diffusion coefficient of electrode *i*	[cm^2 s^{-1}]
$D_{i,k\ (eff)}$	effective Knudsen diffusivity of component *i*	[cm^2 s^{-1}]
$D_{A-B\ (eff)}$	effective ordinary diffusivity of gas A versus gas B	[cm^2 s^{-1}]
E	theoretical open-circuit voltage of the cell	[V]
E_0	theoretical open-circuit voltage of the cell at standard pressure	[V]
E_a	activation energy	[kJ mol^{-1}]
F	Faraday constant (9.6495×10^4)	[C mol^{-1}]
i	current density	[A cm^{-2}]
i_0	exchange current density	[A cm^{-2}]
i_{ave}	average current density	[A cm^{-2}]

J_i	Permeate flux of species *i*	[mol m^{-2} s]
J_0	preexponential factor of Permeate flux	[mol m^{-2} s]
l	membrane thickness	[m]
l_a	thickness of anode electrode	[μm]
l_c	thickness of cathode electrode	[μm]
L	thickness of electrolyte	[μm]
LHV_i	lower heating value of component *i*	[J mol^{-1}]
m_i	molar flow rate of component *i*	[mol s^{-1}]
M_i	molecular weight of gas *i*	[g]
n	electrode porosity	[-]
p_{ave}	average power density	[W cm^{-2}]
p_i	partial pressure of component *i*	[Pa]
p_i^I	inlet pressure of component *i*	[Pa]
P	pressure	[Pa]
P_{ref}	reference pressure (10^5)	[Pa]
Q	thermal energy	[MW]
Q_{net}	net thermal energy	[MW]

R	gas constant (8.3145)	[J mol^{-1} K^{-1}]
T	temperature	[K]
U_f	fuel utilization	[-]
V	cell voltage	[V]
W_e	electrical power	[MW]
$W_{e,net}$	net electrical power	[MW]
W_{pump}	electrical power consumed in pump	[MW]
x_i	mole fraction of component *i* at feed (retentate) side of the membrane	[-]
y_i	mole fraction of component *i* at permeate side of the membrane	[-]
z	number of electron participating in the electrochemical reaction	[-]

Greek letters

α	charge transfer coefficient	[-]
ξ	electrode tortuosity	[-]
δ_{O_2}	coefficient used in concentration overpotential	[-]

η_{act}	activation loss	[V]
η_{conc}	concentration loss	[V]
η_{ohm}	ohmic loss	[V]
η_{pump}	pump efficiency	[-]
σ_{AB}	collision diameter	[Å]
Ω_D	collision integral	[-]
ε_{AB}	Lennard-Jones energy interaction parameter scaled with respect to the Boltzman constant	[-]
γ_a	pre-exponential factor for anode exchange current Density	[A m^{-2}]
γ_c	pre-exponential factor for cathode exchange current Density	[A m^{-2}]

Subscripts

a	anode
c	cathode
0,f	feed side
p	permeate side

CHAPTER I

INTRODUCTION

The rapid growth of economy leads to a high demand of energy especially electrical power in order to support its expansion. Nevertheless, power generation systems at present are mainly based on low-efficiency combustion heat engines which have substantial losses of energy during many energy conversion stages (Douvartzides et al., 2003). According to this reason, one choice of interest is fuel cell technology because it can fulfill the requirement of both effective and clean power generation unit. It converts the chemical energy of hydrogen fuel directly into electrical power and releases steam as a harmless product. Solid oxide fuel cell (SOFC), one type of fuel cells, has offered many advantages, for examples, flexibility of various fuels usage, heat recovery cogeneration, fast kinetic rate and internal reforming. In addition, SOFC can reduce emissions of greenhouse gas and air pollutants causing serious environmental impacts.

Selection of appropriate fuels for fuel cell is a crucial issue. Fuels should be ecological friendly and derived from sustainable energy resources. In contrast, non-renewable fossil fuels should be avoided. Renewable biofuel is available from agricultural products and suitable for countries which have strong agriculture sector. Several renewable fuels have been used for fuel cell such as methane, methanol, biogas, ethanol and ammonia. All of these fuels can be reformed into hydrogen-containing gas. Methane is an attractive choice for fuel cell because of its high hydrogen to carbon ratio (Naidja et al., 2003). Ammonia is another choice since it releases zero-carbon emission (Zhang and Yang, 2008). Biogas has been widely used because it consists of 40-65 mol% methane (Dayton, 2001) high enough to be directly used as a fuel but biogas is based on source scales, normally small-scale, it may be an inconsistent resource. However, it is inevitable that using these fuels may face the problem of carbon deposition when SOFC is operated. Plenty of solutions have been undergone to solve this problem. A simple method is to adjust proper ratio of related compositions or operating conditions to avoid boundary of carbon formation.

Among the various biofuels, bioethanol is a particularly promising fuel due to a number of benefits: high hydrogen content, availability, non-toxicity, ease of handling and storage (Meng Ni et al., 2007). Moreover, bioethanol can be derived from various biomass sources such as sugar cane molasses, lignocelluloses and agroindustrial wastes (Comas et al., 2004) by fermentation processes. The net carbon dioxide emission from bioethanol utilization is lower than fossils (Arteaga-Perez., 2009) because of its carbon-closed cycle. However, bioethanol contains mainly water and dilute ethanol. In order to be an effective fuel for a fuel cell, water must be removed from bioethanol by purification to obtain a higher ethanol concentration which is later reformed into hydrogen rich gas for feeding into SOFCs.

There are several choices for purification processes such as distillation, adsorption, membrane etc. In previous work, the SOFC systems integrated with distillation was examined (Jamsak et al., 2007). It was found that the systems have somewhat low electrical efficiency due to limitation of high reboiler heat duty consumption. Adsorption unit seems to be a low energy consumption system but this unit faces the problem in using plenty of adsorption agents when it operates at large scale. It is difficult to regenerate adsorption agents and to achieve high recovery yield of ethanol (Chang et al., 1998). Pervaporation membrane separation is an interesting choice. As the pervaporation does not depend on thermodynamic equilibrium, it can avoid the azeotropic problem occurred with ethanol/water system. It also requires lower energy consumption compared with a distillation because pervaporation relies on the different ability of each substance which adsorbs and diffuses through membrane material. Although some problems may occur with pervaporation such as high capital cost, thermal instability and short life time, in the energy point of view, SOFC systems produce both electricity and thermal energy. Installing a pervaporation can reduce burden of SOFC unit in case of distributing much thermal energy supplied to purification unit. Instead of heating the separation unit, excess thermal energy can be taken to another added power cogeneraton (combined heat and power, CHP) units like turbine and recuperator to increase the overall efficiency of SOFC systems.

From the reasons mentioned above, this research is emphasized on efficiency analysis of solid oxide fuel cell system fed by bioethanol incorporated with pervaporation unit. Firstly, Selection of appropriate pervaporation membrane type for

the overall system is investigated. After obtaining a suitable membrane type of pervaporation, a performance of the overall system is further improved by installing vapor permeation as an extra separation unit after pervaporation. The appropriate membrane type for vapor permeation is also investigated to serve an optimal efficiency of the system. The electrical efficiencies of the system before and after installing vapor permeation are compared. Finally, SOFC system integrated with the proposed purification process is compared with the use of ordinary distillation column to clearly show its performance improvement.

CHAPTER II

THEORY

2.1 Fuel Cell

2.1.1 Fundamental Principle

A fuel cell is an electrochemical reactor where the chemical energy of fuel gas is directly converted into electricity (DC), heat and water. It consists of three main parts, a cathode (positive electrode), an anode (negative electrode) separated by an electrolyte. It has a current collector which is connected between two electrodes through an external circuit (load). When connecting the cells together in a stack, interconnect plates are used for separating between a cathode of a cell and an anode of the next cell (Minh, 1993). The diagram of a fuel cell is schematically shown in Figure 2.1. Unlike the conventional batteries, fuel cell does not require recharging and can be operated as long as both fuel and oxidant gases are fed into the electrodes. The oxidant gas is fed to the cathode side while the fuel is fed to the anode side releasing electrons from a hydrogen oxidation reaction. Electrons pass through an external circuit, whilst the ions transfer across the electrolyte. The products from this reaction are water and heat.

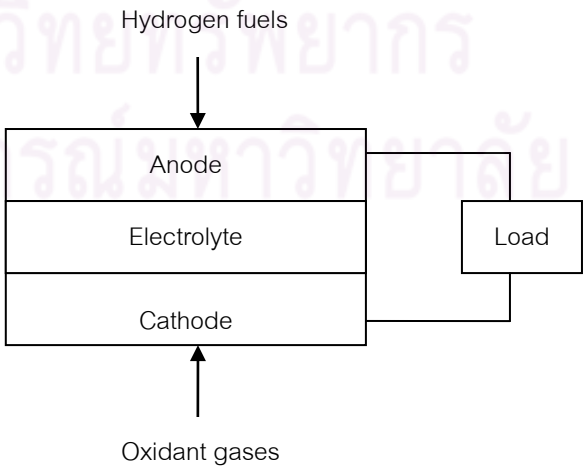

Figure 2.1 The general diagram of a fuel cell

2.1.2 Components of Fuel Cell

A fuel cell fundamentally contains major components of electrolyte, cathode and anode as shown in Figure 2.1. When the cells are stacked together, extra components i.e. interconnect and separator plates are required. The required properties for each component are the followings:

2.1.2.1 Electrolyte

Electrolyte, an ion conducting media, performs as a carrier medium of either oxide-ion or proton. The preferred materials for electrolyte are:

- Low electronic conductivity –electrolyte with high electronic conduction can cause higher voltage loss.
- High ion conductivity
- High mechanical and thermal strength.
- Low gas leakage through an electrolyte

2.1.2.2 Anode/Cathode electrode

For an anode electrode, high electronic conductivity is required for transferring electrons because the reaction occurred on the anode side is oxidation which normally releases electrons. The materials must have thermal expansion compatible with electrolyte and interconnector. Tolerance to impurities in fuel gas is needed for anode materials and it also should have a catalytic property which is essential for a fuel oxidation reaction (Fergus, 2006).

The reduction reaction of an oxidant gas occurred on the cathode to complete its mechanism. The required property for the cathode is high electronic conductivity typically in term of electron receptor. The material used in cathode should contain sufficient porosity for gas transport and structural stability during operation. Also, it is less reactive at the vicinity of the electrolyte and interconnector.

2.1.2.3 Interconnector

The role of interconnector is to separate between the cells which are stacked together. The required properties are:

- High electronic conductivity
- Structural stability and chemical resistance during operation
- Thermal expansion matching with other components
- Chemically compatible with electrolyte and interconnector at operating conditions

2.1.3 Types of Fuel Cells

There are several types of fuel cells categorized by electrolyte materials which are related with anode fuels and operating temperature. The characteristics of these fuel cells are shown in Table 2.1.

Table 2.1 Characteristics of different types of fuel cells

Fuel Cell Type	Electrolyte	Operating temperature (K)	Fuel	Oxidant	Efficiency (%)
AFC	Potassium hydroxide	323-473	H_2 , Hydrazine	O_2 ,air	50-55
DMFC	Proton-exchange membrane	333-393	CH_3OH, H_2O	O_2 ,Humid air	40
PAFC	Phosphoric acid	433-483	H_2	O_2 ,Air	40-50
MCFC	Molten salts i.e. carbonates, nitrates	903-923	H_2 ,CO, CH_4	O_2 , CO_2, Air	50-60
PEFC	Hydrated Polymeric Ion Exchange Membranes	323-353	H_2	O_2 , Air	40-50
SOFC	Fluorite (Ceramics)	873-1273	H_2 ,CO, CH_4	O_2 , Air	45-60

Fuel cells have been used for several applications. The appropriate selection of these fuel cells depends on power requirement in each usage, appropriate size for using areas, operating temperature in term of energy supply. Portable fuel cells such as Alkaline Fuel Cell (AFC), Polymer Electrolyte Fuel Cell (PEFC), and Direct Methanol Fuel Cell (DMFC) have been applied for mobile phone, vehicle, laptop, and electronic devices. For stationary fuel cell namely Phosphoric Acid Fuel Cell (PAFC), Molten Carbonate Fuel Cell (MCFC), and Solid Oxide Fuel Cell (SOFC) are suitable for medium-to-large power generation.

2.1.4 Advantages and Disadvantages of Fuel Cell

Apparently, hydrogen based fuel cell becomes a versatile power generator, releasing both heat and electrical power, that is superior to common power generations. Nonetheless, fuel cells at the present time are still limited in usages due to facing of competitive manufacturing cost and short-life time.

2.1.4.1 Advantages

- Higher efficiency than conventional combustion heat engines. Because of direct energy conversion and no moving part in the energy converter, so it reduces the energy losses in fuel cells.
- Without burning fuels, fuel cell releases only water and help reduce the emission of NO_x, SO_x and particulates to atmosphere.
- Fuel cells can be used in various fuels apart from fossil fuels. The flexibility of fuels takes fuel cells away from limited energy resources.
- Silent operation owing to a lack of moving parts.
- Convenient to supervise since fuel cells mostly consist of stationary parts.
- Able to be an unattended/remote operation.

2.1.4.2 Disadvantages

- Alternative fuels i.e. methanol, biogas and methane require reforming process. During reforming stages, it is possible that this process can release polluted products via utilizing hydrocarbon feeds.

- Technology is still at a level of development. For example, power density obtained from fuel cell is limited and required further improvements if fuel cell is to compete in portable and automotive applications.
- High market entry cost, less competitive capacity than conventional power generations.
- Operational temperature compatibility, durability under start-stop cycling concerns.
- Almost no infrastructure to support fuel cell technology i.e. fuel storage, transportation.

2.2 Solid Oxide Fuel Cell

Solid oxide fuel cell is made of rigid ceramics as electrolyte. This material help SOFC alleviate any corrosion problems from poisonous substances usually occurred in the polymer electrolyte. On the other hand, its tolerance benefits various fuels usage. It operates at high temperature about 873-1,273 K. Due to high temperature operation, it is not necessary to use expensive noble metal as a catalyst and also enhance the fuel reforming within the cell at the anode side. This reduces the complexity of system and capital cost for installing an external reformer. However, operating at high temperature leads to slow energy distributed startup and short-life of SOFC structural material.

2.2.1 Principle of SOFC operation

Generally, SOFC operation can be divided into two types of electrolyte; namely, Oxygen ion conducting electrolyte and Proton conducting electrolyte. The main difference between these electrolytes is the location of water formation produced from fuel cell occurs in opposite cell sides as shown in Figures 2.2 and 2.3

The electrochemical reaction of the SOFC-H^+

Anode : $2H_2 = 4H^+ + 4e^-$ (2.1)

Cathode : $O_2 + 4H^+ + 4e^- = 2H_2O$ (2.2)

Overall : $2H_2 + O_2 = 2H_2O$ (2.3)

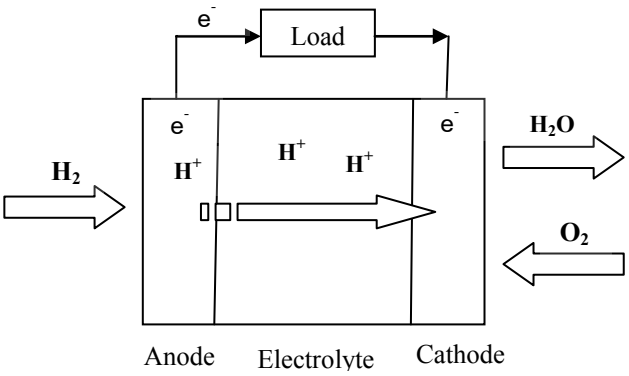

Figure 2.2 Operational principle of SOFC-H^+ operation

The electrochemical reaction of the SOFC-O^{2-}

Anode : $H_2 + O^{2-} = H_2O + 2e^-$ (2.4)

Cathode : $\frac{1}{2}O_2 + 2e^- = O^{2-}$ (2.5)

Overall : $2H_2 + O_2 = 2H_2O$ (2.6)

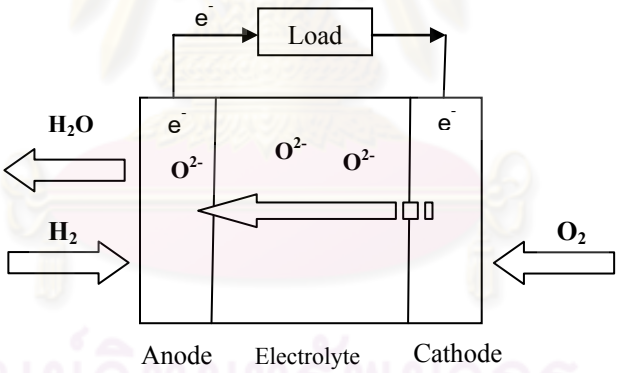

Figure 2.3 Operational principle of SOFC-O^{2-} operation

2.2.2 Characteristics of SOFC

2.2.2.1 Open circuit voltage

Open circuit voltage (OCV) is the maximum ideal voltage that can be carried out when operated at a specific condition. Because of different concentration of components between anode and cathode sides, this causes different potential at the anode and cathode and results in OCV of the fuel cell. Electrons were moved from an electrode to another one and the current was generated.

2.2.2.2 Polarizations

Although the OCV is the theoretical maximum ideal voltage, the actual voltage of SOFC is less than the theoretical voltage value. Owing to the presence of polarizations, polarizations can be classified into four types as follows:

a) Activation Polarization

Activation Polarization is the polarization which occurs from electrochemical reaction at the electrodes. Some energy is required to overcome energy barrier as activation energy for electrochemical reaction, i.e. adsorption of reactant on the electrode surface and desorption of product out of the surface. Normally, activation polarization dominates at low current density regions and the characteristics curve is non-linear. However, at high temperature operation of SOFC, the rate-determining step is very fast resulted in small value of activation polarizations. The linear characteristic curve can be noticed.

b) Ohmic Polarization

Ohmic polarization results from the resistance of ions flow within the electrolyte and resistance of electrons flow through the electrodes. Ohmic polarization is a major loss in the SOFC stack when compared to other losses.

c) Fuel Crossover or Internal Current Polarization

Typically, an electrolyte should permit only ions transported through the cell and no fuel cross over the electrolyte. Although fuel crossing through an electrolyte or electrons leaking to an electrolyte is possible, the fuel crossover loss is very small amount.

d) Concentration Polarization

Concentration polarization is caused by concentration in form of partial pressure in porous electrode region reduce more than bulk gas outside this region. This phenomenon occurs when SOFC operates at high temperature or high fuel utilization. The gradient between the concentrations in each region causes this type of

polarization. At lower current densities and fuel utilization. The concentration polarization is very small.

The overall characteristics of SOFC are summarized as shown in Figure 2.4

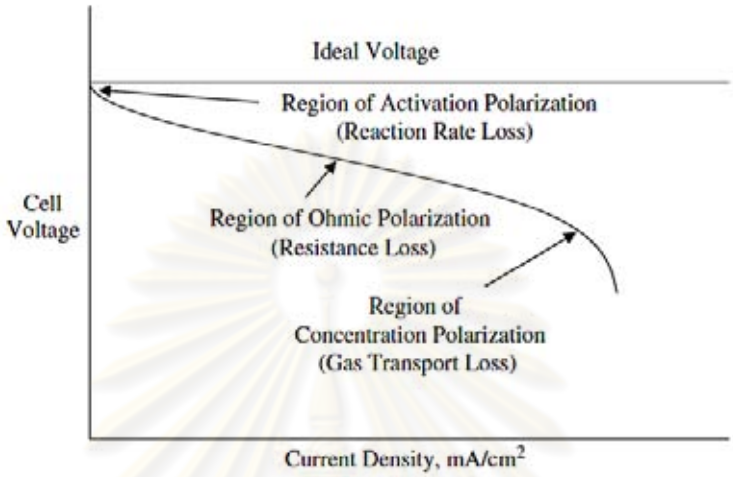

Figure 2.4 Schematic of ideal and actual voltage in a fuel cell (Kakac et al., 2007)

2.2.3 Reforming operation of SOFC

SOFC can be fed with various fuels apart from pure hydrogen i.e. methanol, ethanol, biogas. However, these fuels have to be reformed into hydrogen before being fed to SOFC. There are three modes for SOFC reforming operations; External Reforming (ER), Indirect Internal Reforming (IIR), and Direct Internal Reforming (DIR). Each type of reforming operation is schematically shown in Figure 2.5

a)

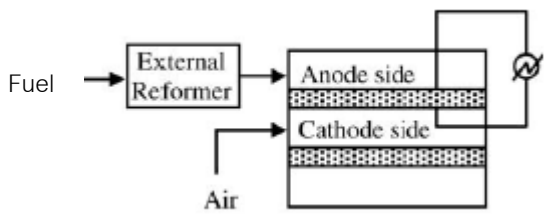

b)

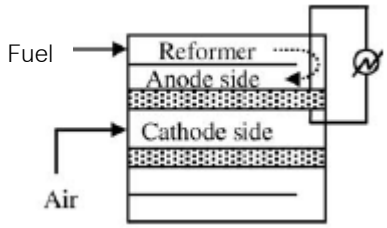

c)

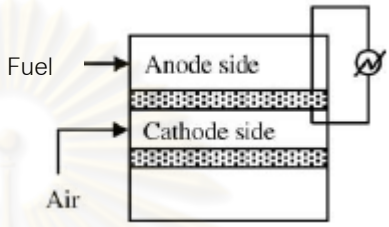

Figure 2.5 Type of reforming operation of SOFC: a) ER-SOFC, b) IIR-SOFC, c) DIR-SOFC

From these types of reforming, the location of reforming section is significantly different. As the electrochemical reaction is exothermic, releasing steam, while the reforming reaction is endothermic, the reaction can transfer heat and steam each other. For ER in Figure 2.5 a), the reforming section and SOFC are completely separated. Heat and steam from SOFC section do not involve reforming section. For IIR in Figure 2.5 b), the reforming section is located next to the SOFC, this structure makes use of the exothermic heat from SOFC section to reforming section except for steam that could not be involved. For DIR in Figure 2.5 c), the reforming and SOFC sections are located together. Therefore, this system can benefit a full advantage of both heat and steam to interchange each other between these reactions.

2.2.4 SOFC System and Balance of Plant

For SOFC power generation system, by installing only SOFC unit is not enough to improve the process performance. Some extra process equipments are provided to support electricity production. These components are called "Balance of Plant (BoP)". Generally, the overall SOFC process can be divided into four sections namely; Fuel processing section, Electric generating section, Heat recovery section and electrical power conditioning as follows:

2.2.4.1 Fuel processing section

The role of this section is to modify the incoming reactants to be in proper conditions before being fed into the SOFC. Conventionally, a fuel is reformed into hydrogen in a reformer separated from SOFC to avoid coke formation within the SOFC. The equipments required for bioethanol in a fuel processing section are described below.

- A pervaporation membrane is used as a separation unit for purifying ethanol to the desired concentration before being fed into the reformer.
- A reformer converts concentration-modified ethanol into hydrogen fuel for the SOFC unit.
- A compressor is used to increase the pressure of the gas stream line to be in a proper condition before being fed into a reformer.
- A vacuum pump is a part of pervaporation unit to create the pressure driving force enhanced separation performance of pervaporation.
- Preheaters are used for modifying temperature of the inlet stream lines of fuel and oxidant feeds to be at a suitable condition.

2.2.4.2 Electrical power generation

This is a major process section in a power generation system. It contains an SOFC unit sequenced after the fuel processing section. The SOFC is fed with bioethanol-derived hydrogen and produces direct current power via electrochemical reaction.

2.2.4.3 Heat recovery section

This section contains heat exchangers and the afterburner to combust residual fuels from electrochemical reaction in SOFC. Thermal power obtained from an afterburner and outlet streams from SOFC is distributed to other equipments requiring some energy supply i.e. reformer, preheaters and other extra power generations in order to reduce the demand of external heat sources and take this power generation to be a worthwhile energy usage.

2.2.4.4 Electrical power conditioning

The electrical power conditioning consists of a unit which converts direct current from SOFC into alternating current for actual usage. In addition, the DC-AC converter is also installed for an added power generation like gas turbine. However, DC-AC inverter is not considered in this study.

2.3 Ethanol reforming reaction

Ethanol as a fuel can be converted into hydrogen. Reforming of ethanol provides a promising method for hydrogen production from renewable sources. Different catalysts such as non-noble metals and noble metals are researched for ethanol reforming. Reforming operation-modes for hydrogen production can be classified into three main types:

- Steam reforming
- Partial oxidation
- Auto-thermal reforming

From these proposed operation modes, selection of each reforming operation is considered from individual objectives. If the main target is to obtain a high yield of hydrogen with low carbon monoxide content, steam reforming operation is a suitable mode but it demands an energy supply due to endothermic reaction. In case of focusing on less system complexity and integration, the exothermic partial oxidation is compatible for these requirements since no external heat source and steam are required (Vourliotakis et al.,2009). However, the hydrogen selectivity of partial oxidation is low. Auto-thermal reforming or oxidative steam reforming is proposed as another choice to improve the hydrogen production. Since it combines steam reforming and ethanol oxidation, its advantages are not only minimum heat input but also high hydrogen production. Characteristics of all reforming modes are summarized in Figure 2.6 (Rabenstein and Hacker, 2008)

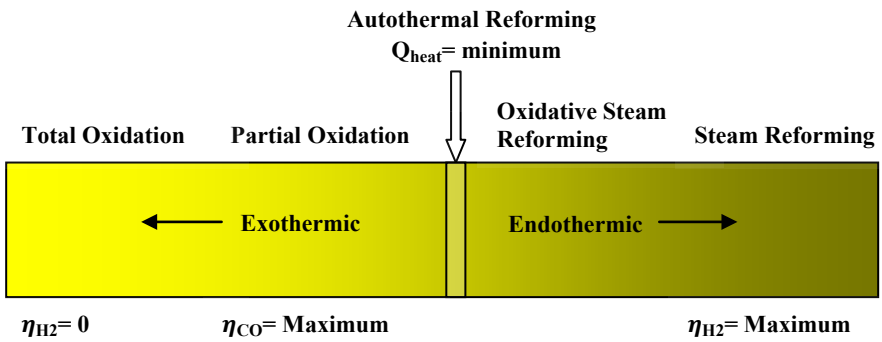

Figure 2.6 Various operating modes of Ethanol reforming

Because ethanol reforming process is considered as a part of fuel processing section and the objective of this research is to obtain hydrogen as high as possible in order to enhance the power generation performance from a fuel cell. The ethanol steam reforming is then selected due to the highest hydrogen yield compared to the other operation modes.

2.3.1 Ethanol steam reforming

The studies on steam reforming method are of interest by a number of researchers. Ethanol steam reforming appears at higher temperatures compared to methanol steam reforming and also releases higher carbon monoxide amounts in the outlet stream (Amphlett et al., 1981). Because the target is to maximize hydrogen selectivity and inhibit coke formation, the selection of a suitable catalyst plays a crucial role due to each catalyst induces different pathways. Rh and Ni –noble metal and non-noble metal catalysts- are the best and the most commonly used catalysts for ethanol steam reforming (Meng Ni et al., 2007). In practice, there are a number of possible reaction pathways of ethanol steam reforming to be described as follows:

In case of the process having a sufficient steam supply, the ethanol steam reforming reaction is

$$C_2H_5OH + 3H_2O \rightarrow 6H_2 + 2CO_2 \quad (\Delta H^o_{298} = +173.5 \text{ kJ/mol}) \qquad (2.7)$$

The equation (2.7) gives the highest hydrogen production and it is a desired pathway. If the steam is supplied to the process insufficiently, the undesired reactions may occur

$$C_2H_5OH + H_2O \rightarrow 4H_2 + 2CO \quad (\Delta H^o_{298} = +256 \text{ kJ/mol}) \quad (2.8)$$

$$C_2H_5OH + 2H_2 \rightarrow 2CH_4 + H_2O \quad (\Delta H^o_{298} = -157 \text{ kJ/mol}) \quad (2.9)$$

These reactions release a lower hydrogen production including byproducts. In addition, the other reactions regarding to ethanol can be occurred namely:

<u>Dehydrogenation</u>

$$C_2H_5OH \rightarrow CH_3CHO + H_2 \quad (\Delta H^o_{298} = +68 \text{ kJ/mol}) \quad (2.10)$$

This is another reaction pathway for hydrogen production in practice. However, acetaldehyde occurred can be further reacted by two reactions:

- Acetaldehyde decomposition

$$C_2H_4O \rightarrow CH_4 + CO \quad (\Delta H^o_{298} = -21 \text{ kJ/mol}) \quad (2.11)$$

- Acetaldehyde steam reforming

$$C_2H_4O + H_2O \rightarrow 3H_2 + 2CO \quad (\Delta H^o_{298} = +180 \text{ kJ/mol}) \quad (2.12)$$

<u>Dehydration</u>

$$C_2H_5OH \rightarrow C_2H_4 + H_2O \quad (\Delta H^o_{298} = +45 \text{ kJ/mol}) \quad (2.13)$$

The dehydration of ethanol is an undesired pathway which is the main source of coke formation according to this reaction:

$$C_2H_4 \rightarrow \text{polymeric deposits (coke)} \quad (2.14)$$

Decomposition

$C_2H_5OH \rightarrow CO + CH_4 + H_2$ (ΔH^o_{298} = +49 kJ/mol) (2.15)

$2C_2H_5OH \rightarrow C_3H_6O + CO + 3H_2$ (ΔH^o_{298} = 98 kJ/mol) (2.16)

$C_2H_5OH \rightarrow 1/2CO_2 + 3/2CH_4$ (ΔH^o_{298} = -74 kJ/mol) (2.17)

Reaction of decomposition products can be converted to methane via the following reactions

$CO + 3H_2 \rightarrow CH_4 + H_2O$ (ΔH^o_{298} = -210 kJ/mol) (2.18)

$CO_2 + 4H_2 \rightarrow CH_4 + 2H_2O$ (ΔH^o_{298} = -160 kJ/mol) (2.19)

The decomposition of ethanol gives a low hydrogen production and may lead to the appearance of coke formation due to carbon monoxide and methane products as following reactions:

- Methane decomposition

$CH_4 \rightarrow 2H_2 + C$ (ΔH^o_{298} = +75 kJ/mol) (2.20)

- Boudouard reaction

$2CO \rightarrow CO_2 + C$ (ΔH^o_{298} = -171.5 kJ/mol) (2.21)

Nonetheless, there are several reactions which obstruct pathways for hydrogen production. The water gas shift reaction can enhance hydrogen production and reduces coke formation.

$CO + H_2O \rightarrow CO_2 + H_2$ (ΔH^o_{298} = -41.32 kJ/mol) (2.22)

2.4 Pervaporation Membrane

2.4.1 Fundamental Principle

Pervaporation is a membrane-based separation process to separate liquid mixture using different ability of each liquid which dissolves and diffuses through a dense, non-porous membrane relying on a physical-chemical affinity between the membrane material and the species. As illustrated in Figure 2.7, a liquid feed mixture is in contact with one side of the membrane. In the membrane section, absorbed liquids are under VLE condition and all partial vapor pressure are at saturation. The driving force of pervaporation is the pressure gradient between the feed and the permeate side of the membrane created by vacuum pump or an inert purge stream in order to reduce permeate side partial vapor pressure. The permeate product through the membrane followed by evaporation is removed as a low pressure vapor into another side and then condensed to liquid state.

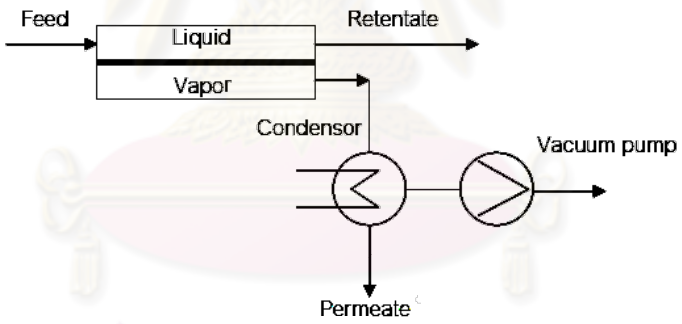

Figure 2.7 The schematic diagram of a pervaporation process

2.4.2 Characteristics and Important terms of Pervaporation

2.4.2.1 Permeation flux

Permeation flux strongly depends on the feed composition, permeate pressure and temperature of the process (Kujawski, 2000). The permeation involves phase change of the permeating species and can result in significant temperature drop at high

permeation rate. From experimental data, the temperature dependence of the permeation flux is commonly expressed as Arrhenius-type relation.

$$J = J_o \exp(-E_a/RT) \tag{2.23}$$

where E_a is defined as an activation energy for permeation. However, this equation is not entirely correct because it does not correspond to any other research dealing with this phenomenon (Feng and Huang, 1997). The flux equation can be derived based on the solution-diffusion model.

$$J_i = \frac{P_i}{l}(p_{io} - p_{ip}) \tag{2.24}$$

where p_{io} and p_{ip} are the partial vapor pressures i on the feed and permeate sides of the membrane, respectively. l is the membrane thickness, and P_i is the permeability. p_{io} can be written in another term dealing with vapor-liquid equilibrium (VLE) condition in a membrane phase as follows:

$$J_i = \frac{P_i}{l}(\gamma_{io}^L x_{io}^L p_{io}^{sat} - p_{ip}) \tag{2.25}$$

where γ_{io}^L is the activity coefficient of component i on the liquid feed side, x_{io}^L is liquid mole fraction of component i in the feed side and p_{io}^{sat} is the saturated vapor pressure of pure component i.

2.4.2.2 Membrane separation factor

This parameter is the ratio of the mole fractions of desired component A and undesired component B in the permeation and feed sides of membrane.

$$\alpha_{AB} = \frac{y_A / y_B}{x_A / x_B} \tag{2.26}$$

2.4.2.3 Membrane permeability

Permeability is the coefficient with respect to the driving force exhibited in terms of partial pressure and is related to the sorption coefficient (K_i) and membrane diffusion coefficient (D_i):

$$P_i = D_i K_i = J_i \frac{l}{p_{io} - p_{ip}} \tag{2.27}$$

where K_i and D_i usually depend on temperature. The relationship of these two parameters and temperature can be expressed as Arrhenius-type relationship. Normally, the permeability is reported as Barrers.

2.4.2.4 Membrane permeance

When the membrane thickness is unknown, membrane permeance – a component flux divided by driving force, can be used. Permeance unit is defined as gas permeation unit (gpu)

$$\frac{P_i}{l} = \frac{D_i K_i}{l} = \frac{J_i}{p_{io} - p_{iP}} \tag{2.28}$$

2.4.2.5 Membrane selectivity

This parameter is defined as the ratio of the permeabilities or permeances of components i (desired component) and j (undesired component) through the membrane:

$$\beta_{ij} = \frac{P_i}{P_j} = \frac{P_i / l}{P_j / l} \tag{2.29}$$

2.4.2.6 Recovery

Recovery is defined as the ratio of mass of desired component i in the permeate stream to that in the feed stream (Mulder, 1996).

$$\text{Recovery} = \frac{m_{i,p}}{m_{i,f}} \tag{2.30}$$

2.4.2.7 Concentration factor

Concentration factor (CF) is defined as the ratio of molar (or mass) fraction of desired component i in the permeate stream to that in the feed stream (Soni et al., 2009).

$$\text{CF} = \frac{x_{i,p}}{x_{i,f}} \tag{2.31}$$

2.4.3 Practical Applications of Pervaporation

At present, an overview of the potential practical applications of pervaporation is classified into three main areas (Kujawski, 2000):

2.4.3.1 Separation of water from aqueous mixtures

For the removal of water from water/organic liquid, hydrophilic membrane materials have to be selected. The hydrophilic property is caused by groups present in the polymer chain are able to interact with water molecules. Examples of hydrophilic membrane materials are: ionic polymers, polyacrylonitryle (PAN), polyvinylalcohol (PVA) and polyvinylpyrrolidone (PVPD). The industrial dehydration processes that can be separated by pervaporation are:

- Dehydration of water-organic azeotropes such as water-ethanol, water-isopropanol and water-pyridine.
- Dehydration of organic reaction in term of enhancement of the chemical reaction efficiency. There are many organic reactions which can release water as one of the products. Examples of such reactions are: esterification reaction, acetalisation and ketalisation. Removal of water can shift the reaction equilibrium toward and obtain more organic products.

2.4.3.2 Removal of organic compounds from aqueous mixtures

For separation of organics from water/organic liquid, hydrophobic polymers are proper membrane property to be chosen. These materials possess no groups that show affinity for water. Examples of these polymers are: polydimethylsiloxane (PDMS), polyethylene (PE), polypropylene (PP), polyvinylidenefluoride (PVFD) and polytetrafluoroethylene (PTFE). Normally, this process is mostly applied for pollution control such as removal of volatile organic compounds (VOCs) from aqueous because VOCs is a source of air pollution and groundwater pollution. Pervaporation can be used for effectively removing VOCs from water by using specially designed hydrophobic membrane i.e. organophilic membrane. In addition, other applications of pervaporation for removing organics are: separation of bioethanol from fermentation broth, removal of chlorinated hydrocarbons, wine and beer dealcoholization, recovery of high-value aroma compounds (flavors, fragrances, and essential oils) from aqueous or alcohol solutions.

2.4.3.3 Separation of Organic-Organic liquid mixtures

For the mixture of two organic liquids, three kinds of mixtures can be differentiated: polar/non-polar, polar/polar and non-polar/non-polar mixtures. Membrane material has to be selected depending on which types of component – polar or non-polar, to remove through the membrane. For the same type mixtures like polar/polar or non-polar/non-polar, it is difficult to separate. The separation has to take place on the criteria of differences in molecular size and shape. Membranes must be custom-designed for specific process objectives. Membrane material such as ceramics has been used as the selective barriers in pervaporation. There are many of organic/organic mixtures which can be separated by pervaporation: Separation of azeotropes (ethanol/cyclohexane, ethanol/ETBE, methanol/MTBE), Separation of isomers (xylenes), aromatics/parafins (benzene/hexane, isooctane/hexane), olefins/parafins (pentene/pentane) and purification of dilute streams (isopropyl alcohol from heptane/hexane).

CHAPTER III

LITERATURE REVIEWS

3.1 Purification process of Ethanol/Water mixture for SOFC system

The distillation column was incorporated into the SOFC system designed by Jamsak et al. (2007) to purify ethanol from dilute bioethanol solution in order to obtain an appropriate composition for SOFC fuel feed. The bioethanol feed at 5mol% was introduced to the distillation column before feeding into a reformer and SOFC stack, respectively. The later two units were assumed to operate under isothermal condition. In this work, the ethanol concentration of 25 mol% was considered as a suitable concentration for ethanol steam reforming reaction producing high hydrogen rich gases. Thermodynamic assessment of the system was investigated, especially focusing on distillation energy consumption. The simulations were conducted under self-sustained energy operation condition (Q_{net}=0) to perform overall electrical efficiency and other essential results. Adjusting SOFC system configurations such as operating voltage and fuel utilization could obtain no external energy demand for the operating condition. For a distillation column, the ethanol recovery at 80% could offer an optimal electrical efficiency under Q_{net}=0. Nonetheless, the designed SOFC system at that condition gained somewhat low performance (0.32 W/cm^2, 173.07 kW, overall electrical efficiency is 33.3% at U_f = 80%, R_{EtOH} = 80% and C_{EtOH} = 41%) owing to high reboiler heat duty consumption. Furthermore, a large amount of heat in a condenser was not recovered. Therefore, it was necessary to have some methods to improve the performance of SOFC-Distillation system.

Afterwards, Jamsak et al. (2009) studied the use of a heat exchanger network for improving the performance of SOFC system integrated with the distillation column. The system utilized exothermic heat from a condenser and hot water from the bottom line of distillation column including cathode recirculation from the cathode outlet stream to supply the energy demanding units. The MER (maximum energy recovery) network was designed to avoid the pinch problem related to the air inlet temperature. The results were found that by eliminating the high temperature distillate

heat exchanger, the total cost index could be reduced. The performance obtained from this modified SOFC system gave the overall electrical efficiency of 40.8%, 54.3% Combined Heat and Power (CHP) efficiency, respectively, as well as 0.221 W/cm^2 for power density.

After discovering the faults when using a distillation column, a low-energy pervaporation was proposed instead of the previous purification unit for bioethanol-fuelled SOFC system to improve the performance as investigated by Choedkiatsakul et al. (2011). This study presented significantly an improvement of SOFC system performance by comparing with two different purification units. At the based case (Q_{net}=0, R_{EtOH} = 80%, Operating voltage = 0.7V, T_{SOFC} = 1073 K), the results showed that the overall electrical efficiency obtained from using the pervaporation offered 42% compared to 34% of distillation column integrated with the system. However, the results indicated that the ethanol separation factor at high values were required when a pervaporation was operated at high ethanol recovery to achieve its high performance. Therefore, it should be concerned on the availability of the pervaporation membrane materials in a later study.

3.2 Pervaporation for Ethanol/Water separation

Among the various separation technologies, membrane-based pervaporation is an interesting alternative because of its high separation efficiency with low energy consumption. Kumar et al. (2010) showed the energy requirements of purification processes i.e. Distillation processes (Azeotropic, Low pressure, Extractive distillation), Solvent extraction and pervaporation for producing anhydrous ethanol. It was found that pervaporation was regarded as being the lowest energy consumption unit compared to the other processes. Pervaporation membrane materials consist of hydrophobic and hydrophilic types. Normally, the component which has smallest amount in the mixture should be permeated across the membrane due to energy saving. Thus, a selection of an appropriate membrane type depends on the property of that component between polar and non-polar. For improving pervaporation membranes, the critical issues to be concerned are: membrane productivity, membrane selectivity and membrane stability (Feng and Huang, 1997). Former research mostly studied the development of membrane materials for dehydration of ethanol/water

system more than ethanol removal from aqueous solution. Due to the growing of research interest in application of biotechnology i.e. removal of ethanol from fermentation broths, developing of membrane materials for dilute ethanol removal has increased gradually. Generally, hydrophobic membranes for ethanol removal are constructed with silicone rubber or polydimethylsiloxane (PDMS). There are several research which study the modified PDMS membrane performance with different nanocomposites. Huang et al. (2009) developed pervaporation membrane for ethanol removal by incorporating polyphosphazene nanotube (PZSNTs) into polydimethylsiloxane (PDMS) to form nanocomposite membranes. SEM showed that PZSNTs were well dispersed in PDMS. The results exhibited higher separation factor than PDMS membranes. From these experiments, as PZSNT content increased from 0% to 10%, the permeation flux and separation factor increased. After this range, both parameters were kept rather unchanged. A decrease of PZSNT diameter leads to an increase in both permeation flux and separation factor. In this study, it was found that by using PZSNT which was adjusted to longest and smallest diameter of nanotube (50 μm and 40 nm) loading at 6 wt% on PDMS could give the maximum separation factor value of 10 compared to 5 (10 wt% ethanol feed at 313 K) from PDMS alone.

High-silica ZSM-5 zeolites (HiSiZ) were filled into PDMS polymers to form mixed matrix membranes by Vane et al. (2008). Several parameters including siloxane chain length, crosslinking agent concentration, density of reactive groups, catalyst level, zeolite type and loading, solvent type, mixing method, and size of a porous support membrane (UF and MF) were studied to assess the effect on pervaporation performance. According to this study, there were three parameters having a significant membrane performance: uniform zeolite particle dispersion, high zeolite loading, zeolite particle size (particularly as it is related to particle agglomeration). It was indicated that the membranes prepared with PDMS system based on DMS-V41/HMS-064 with hydride to vinyl equivalent ratio of 1.34 in case of varying zeolite loadings ranging from 0 to 65wt% had an interesting result. Ethanol-water separation factor increased steadily with zeolite loading from 8.7 at 0wt% to 43.1 at 65 wt% zeolite (5wt% ethanol feed, 323 K, permeate pressure 400-500 Pa).

Lin et al. (2003) investigated the preparation of silicalite membrane which involved in membrane separation properties. Silicalite membrane was synthesized by

in situ crystallization to obtain highly selective silicalite membrane on porous tubular supports. The properties of membrane separation were varied by changing the preparation conditions: seeding, support types, silica sources and temperature. The results reported that the silicalite membranes gave a higher separation selectivity using colloidal silica. The highest ethanol separation factor from this experiment was 106 and flux of 0.9 kg/m^{2}h for 5 wt% ethanol feed at 333 K.

Claes et al. (2010) successfully applied Silica-filled poly(1-trimethylsilyl-1-propyne) (PTMSP) layers on the top of ultrafiltration support membranes and used in the pervaporation of ethanol/water mixtures. From the experiments, Reduction of the thickness of the separating PTMSP top layer and addition of hydrophobic silica particles resulted in a clear flux increase as compared to dense PTMSP membranes. The values of ethanol/water separation factors up to 12 were obtained and fluxes up to 3.5 kg/m^{2}h for 10 wt% ethanol at 323 K. In addition, the supported PTMSP-silica nanohybrid membranes prepared in this work performed even better than the best commercially available organophilic pervaporation membranes in terms of ethanol selectivity and flux. Characteristics of a polyvinylidene fluoride (PVDF) and a polyacrylonitrile (PAN) support membrane disclosed a more open structure for PVDF membrane and showed more hydrophobic surface. From the study, it was suggested that by using a PVDF support, the permeate fluxes can be increased by 30% compared to the PAN supported membranes. Because of their promising flux-selectivity combination, the prepared composite of PTMSP-silica membranes exhibited a great potential in the removal of alcohols from aqueous mixtures and give a new perspective on the removal of alcohols from aqueous streams, and could serve as an alternative for the commercial organic pervaporation membranes.

Pervaporation for product recovery from biomass fermentation processes was reviewed by Vane (2005). The literature stated that the separation factors of PDMS, PTMSP, composite membranes and zeolite are in the range of 4.4-10.8, 9-26, 7-59, 12-106, respectively. However, some research reported that the ethanol/water separation factors could exceed these ranges. For example, Nomura et al. (2002) used silicate zeolite membrane for ethanol removal from the fermentation broth of 20wt% ethanol. The obtained ethanol concentration was 98.2 wt% at the permeate side. The separation factor of ethanol over water is equal to 218 at 303 K. This high ethanol

selectivity was due to the salt effect in fermentation broth. Separation technologies for biorefinery were reviewed by Huang et al. (2008). In the section of hydrophobic membrane for ethanol removal, they concluded that the ethanol/water separation factors are ranked in the following order: PDMS< PTMSP < composite membranes < zeolite membranes. Although zeolite membranes are more expensive than polymer membranes, it has higher separation factors and flux than others.

3.3 Vapor permeation for Ethanol/Water separation

Apart from the use of pervaporation in Ethanol/Water separation, membrane separation techniques also have vapor permeation which is another proficient separation unit to separate Ethanol/Water mixture. Since the transferring mechanism of component vapor in this unit has no phase change across the membrane, it can reduce the effect of concentration polarization occurring on the feed boundary layer and no temperature drop happened along the membrane (Ito, 1997). In addition, it can prolong the membrane life time as a result of low degree of membrane swelling.

Hayashi et al. (2000) proposed a vapor permeation that was incorporated into ethanol concentration process, obtaining dilute ethanol from the biomass alcoholic fermentation broth to further purify ethanol solutions sequenced from adsorption-desorption process and ethanol stripping column, respectively. Asymmetric polyimide membranes were used for vapor permeation to concentrate ethanol solutions from 30 to 99.6 wt% with ethanol recovery more than 98%. The optimum operating factors, operating conditions and the required membrane area were determined based on the numerical model. The simulation results indicated that the two-stage vapor permeation system could offer a desired concentrated ethanol with high ethanol recovery. Although the system required larger membrane area, the membrane area increased only about 10% compared to that of the single-stage system.

Ethanol dehydration using hybrid distillation-membrane process was investigated by Huang et al. (2010). A simple stripper column was used to purify dilute ethanol from 5 wt% to 50 wt% at the overhead column. Then, the obtained ethanol solutions was further purified with two cascade vapor permeation units achieving ethanol concentration at 90 wt% and 99.7 wt%, respectively. As the

membrane in this process should be stable in ethanol/water mixture under the operating temperatures up to 403 K, this work then investigated the development of perfluoro polymer membranes to serve its conditions. Hydrophobic perfluoro polymers were considered because of their chemical and thermal stability which can be used at high temperature, especially up to 403 K. However, the water permeances of this membrane were quite low, compared with the cross-linked hydrophilic membranes. Thus, multilayer composite membranes combined with hydrophobic perfluoro and hydrophilic membrane were proposed. These membranes have a good thermal stability as well as high water permeances and good selectivity.

CHAPTER IV

MODELING

This chapter describes all related simulation models and procedures of calculation including SOFC system and bioethanol pretreatment processes. VBA (Visual Basic for Application) on Excel spreadsheet was used for simulating the SOFC system to assess overall performance while the purification units i.e. pervaporation and vapor permeation were investigated using preliminary calculations on Excel spreadsheet. The distillation column was simulated using Aspen Plus to evaluate its performance.

4.1 Bioethanol Pretreatment Process

Bioethanol, a part of several renewable resources, was selected to be a fuel feed for SOFC system. As mentioned earlier, bioethanol derived from fermentation broth contains mainly water. In this research, bioethanol feed is assumed to consist of only ethanol and water. It is specified at 10 wt% or 4.16 mol% ethanol at ambient condition in accordance with a range of actual bioethanol containing about 5-12 wt% ethanol (S. Ramaswamy et al., 2008) before being fed into a pretreatment unit as follows:

4.1.1 Preliminary Calculations of Pervaporation and Vapor Permeation

Performance assessment of pervaporation and vapor permeation is conducted under a basic calculation to present the primary results. Various parameters and their criteria were considered based on theory. To reduce the complexity, this calculation defines the ethanol recovery parameter representing the influence from other significant parameters on membrane separation as shown in Eq. (4.1).

$$R_{\mathrm{EtOH}} = f^{n}(T_{\mathrm{Feed}}, \text{membrane area, feed composition, permeate side conditions,}\ldots) = \frac{y_{p(EtOH)}P}{x_{F(EtOH)}F} \quad (4.1)$$

The mass balance equations of pervaporation and vapor permeation are determined as

$$F = P + R \tag{4.2}$$

$$x_{F_i}F = y_{p_i}P + x_{R_i}R \tag{4.3}$$

where F is the total feed, P is the permeate stream, R is the retentate stream, while x_i and y_i represent molar fraction of species i of the retentate and permeate, respectively.

The separation factor as a performance indicator of membrane is another parameter to be employed in the calculation incorporated with ethanol recovery as shown below:

$$\propto_{i/j} = \frac{y_i/y_j}{x_i/x_j} \tag{4.4}$$

In this set of equations, the ethanol concentration of 25 mol% is specified at the permeate stream and retentate stream for hydrophobic and hydrophilic membrane types, respectively. Thereafter, the calculated separation factor values in each type are then obtained including the mass flow rate of permeate and retentate streams. For energy calculation, there are different between pervaporation and vapor permeation. In a pervaporation, heat utilized from sensible heat of liquid feed mixture is necessary for vaporizing a preferential component to be permeated through the membrane. However, the temperature drop is neglected to simplify the calculation. According to the pervaporation, the operating temperatures are limited to below 373 K (R. Smith, 2005), this pervaporation module is defined to operate at 348 K under isothermal condition. The total required thermal energy is shown by the following equation:

$$Q = m\int_{T_{in}}^{T_{out}} C_p dT + mL \tag{4.5}$$

For vapor permeation, thermal energy is required only for the first term of Eq. (4.5) since there is no phase change in the separation mechanism. There are many methods for generating a driving force for the membrane separation. A vacuum pump is considered in this study and is installed in a permeate side to drive chemical potential gradient through the pressure difference. The electrical power required for operating the vacuum pump is calculated by using Eqs. (4.6) and (4.7), respectively.

$$T_{out} = T_{in}\left[1 + \frac{1}{\eta_{pump}}\left[\left(\frac{P_{out}}{P_{in}}\right)^{\frac{\gamma-1}{\gamma}} - 1\right]\right] \quad (4.6)$$

$$W_{e,PV} = -m_p \int_{T_{in}}^{T_{out}} C_p dT \quad (4.7)$$

where $$\gamma = \frac{C_p}{C_p - R} \quad (4.8)$$

The electrical efficiency of a vacuum pump was specified at 75% (T. Kaneko et al., 2006).

4.1.2 Distillation Column

A distillation column which was used as a bioethanol purification unit for the SOFC system in the previous work (Wassana Jamsak et al., 2007) was considered to compare its performance of SOFC system with the proposed purification process-integrated SOFC system of this work under the same conditions to demonstrate its performance improvement. The procedure of bioethanol pretreatment using an ordinary distillation column to obtain a desired concentration is depicted in Figure 4.1.

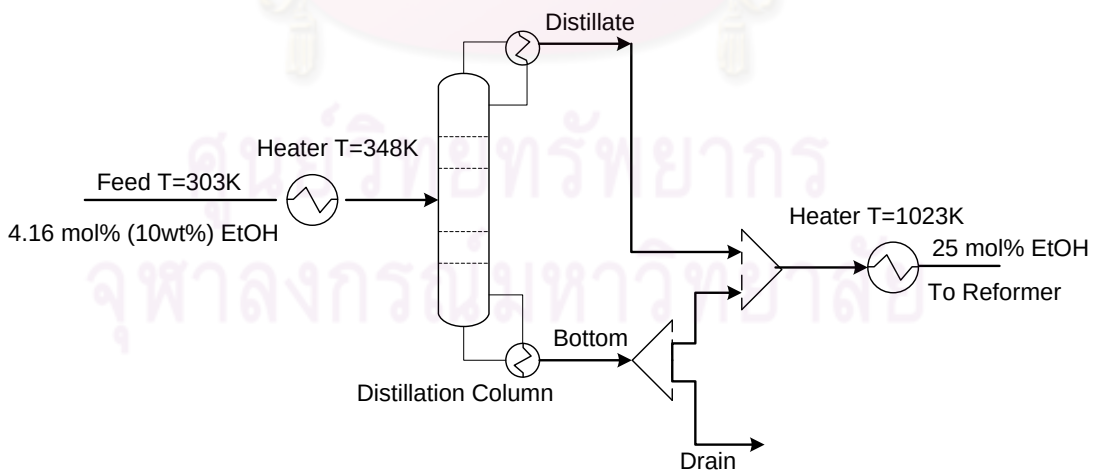

Figure 4.1 The schematic diagram of ordinary distillation column

4.2 SOFC model

The SOFC model was applied from the previous literature (Pakorn Piroonlerkgul et al., 2008) to investigate the overall performance of SOFC system. In this model, a constant operating voltage along the cell length and isothermal condition were assumed. Only hydrogen oxidation was considered to react electrochemically within the module. Oxygen ion electrolyte type was selected for SOFC and its electrochemical reaction occurring as follows:

$$1/2O_2 + 2e^- \rightarrow O^{2-} \tag{4.9}$$

$$H_2 + O^{2-} \rightarrow H_2O + 2e^- \tag{4.10}$$

The verification of the model was in good agreement with experimental results of Zhao et al., (2005) and Tao et al., (2005) at high hydrogen contents (hydrogen mole fraction = 0.97) and Petruzzi et al. (2003) at low hydrogen contents (hydrogen mole fraction = 0.26). The materials used in SOFC stack are YSZ, Ni-YSZ and LSM-YSZ for electrolyte, anode and cathode, respectively.

4.2.1 Electrochemical model

4.2.1.1 Open circuit voltage

The open circuit voltage (E) is calculated by the Nernst equation as given in Eq. (4.11)

$$E = E_0 + \frac{RT}{F}\ln\left(\frac{P_{H_2}P_{O_2}^{1/2}}{P_{H_2O}}\right) \tag{4.11}$$

The actual operating voltage (V) is less than the open circuit voltage (E) due to the presence of polarizations. Three types of polarization are considered in this model: Ohmic, Activation, and Concentration polarizations as below:

$$V = E - \eta_{act} - \eta_{ohmic} - \eta_{conc} \tag{4.12}$$

4.2.1.2 Polarizations

- Ohmic polarization

This polarization involves the resistance of both ions which flow in the electrolyte and electrons which flow through the electrodes. This resistance loss is regarded as a major loss in the SOFC stack and is given as:

$$\eta_{ohmic} = 2.99x10^{-11} iL \exp\left(\frac{10300}{T}\right) \quad (4.13)$$

- Activation polarization

Activation polarization is caused by the loss of electrochemical reaction rate at the electrodes. An operation of SOFC at high temperature can reduce this polarization as the rate-determining step becomes faster. Normally, activation polarization region locates at low current density range. This polarization is defined by Butler-Volmer equation.

$$i = i_0\left[\exp\left(\frac{\alpha zF\eta_{act}}{RT}\right) - \exp\left(-\frac{(1-\alpha)zF\eta_{act}}{RT}\right)\right] \quad (4.14)$$

The value of α and z are specified as 0.5 and 2 (S.H. Chan et al., 2001), respectively. Accordingly, the activation polarization at anode and cathode sides can be arranged into another form as:

$$\eta_{act,j} = \frac{RT}{F}\sinh^{-1}\left(\frac{i}{2i_{0,j}}\right) \quad \text{, j = anode, cathode} \quad (4.15)$$

The exchange current density ($i_{0,j}$) for both the anode and cathode sides are expressed as follows:

$$i_{o,a} = \gamma_a\left(\frac{P_{H_2}}{P_{ref}}\right)\left(\frac{P_{H_2O}}{P_{ref}}\right)\exp\left(-\frac{E_{act,a}}{RT}\right) \quad (4.16)$$

$$i_{o,c} = \gamma_c \left(\frac{P_{O_2}}{P_{ref}} \right)^{0.25} \exp\left(-\frac{E_{act,c}}{RT} \right) \tag{4.17}$$

- Concentration polarization

This polarization results from a partial pressure in porous electrode region reduce more than bulk gas outside this region and is brought to a gas transport loss. It can be estimated by Eqs. (4.18) and (4.19) for anode and cathode sides, respectively.

$$\eta_{conc,a} = \frac{RT}{2F} \ln\left[\frac{\left(1 + (RT/2F)(l_a / D_{a(eff)} p^I_{H_2O})i\right)}{(1 - (RT/2F)(l_a / D_{a(eff)} p^I_{H_2})i} \right] \tag{4.18}$$

$$\eta_{conc,c} = \frac{RT}{4F} \ln\left[\frac{p^I_{O_2}}{(p_c/\delta_{O_2}) - ((p_c/\delta_{O_2}) - p^I_{O_2}) \exp\left[(RT/4F)(\delta_{O_2} l_c / D_{c(eff)} p_c)i\right]} \right] \tag{4.19}$$

where δ_{O_2}, $D_{a(eff)}$ and $D_{c(eff)}$ are given by:

$$\delta_{O_2} = \frac{D_{O_2,k(eff)}}{D_{O_2,k(eff)} + D_{O_2-N_2(eff)}} \tag{4.20}$$

$$D_{a(eff)} = \left(\frac{p_{H_2O}}{P_a} \right) D_{H_2(eff)} + \left(\frac{p_{H_2}}{p_a} \right) D_{H_2O(eff)} \tag{4.21}$$

$$D_{c(eff)} = \frac{\xi}{n} \left(\frac{1}{D_{O_2,k}} + \frac{1}{D_{O_2-N_2}} \right) \tag{4.22}$$

$$\frac{1}{D_{H_2(eff)}} = \frac{\xi}{n} \left(\frac{1}{D_{H_2,k}} + \frac{1}{D_{H_2-H_2O}} \right) \tag{4.23}$$

$$\frac{1}{D_{H_2O(eff)}} = \frac{\xi}{n} \left(\frac{1}{D_{H_2O,k}} + \frac{1}{D_{H_2-H_2O}} \right) \tag{4.24}$$

The relationship between the effective diffusion parameter ($D_{(eff)}$) and ordinary diffusion parameter (D) can be described by:

$$D_{(eff)} = \frac{n}{\xi} D \tag{4.25}$$

Assuming straight and round pores, the Knudsen diffusion parameter can be calculated by:

$$D_{A,k} = 9700\sqrt{\frac{T}{M_A}} \tag{4.26}$$

The binary ordinary diffusion parameter in a gas phase can be calculated using the Chapman-Enskog theory of prediction as below:

$$D_{A-B} = 1.8583x10^{-3}\left(\frac{T^{3/2}((1/M_A)+(1/M_B))^{1/2}}{P\sigma_{AB}^2\Omega_D}\right) \tag{4.27}$$

where σ_{AB} is the characteristic length and Ω_D is the collision integral. These parameters are given by:

$$\sigma_{AB} = \frac{\sigma_A + \sigma_B}{2} \tag{4.28}$$

$$\Omega_D = \frac{A}{T_k^B} + \frac{C}{\exp(DT_k)} + \frac{E}{\exp(FT_k)} + \frac{G}{\exp(HT_k)} \tag{4.29}$$

where the constants A to H are A = 1.06036, B = 0.15610, C = 0.19300, D = 0.47635, E = 1.03587, F = 1.52996, G = 1.76474, H = 3.89411 and T_k is given as

$$T_k = \frac{kT}{\varepsilon_{AB}} \tag{4.30}$$

where k is the Boltzmann constant and ε_{AB} is the characteristic Lennard-Jones energy.

All the parameters used in this model are concluded in Table 4.1

Table 4.1 Summary of all parameters used in the SOFC model

Parameters	Value	Parameters	Value
L (μm)	50	σ_{H_2} (Å)	2.827
$E_{act,a}$ (J/mol)	1.0 x 10^5	σ_{H_2O} (Å)	2.641
$E_{act,c}$ (J/mol)	1.2 x 10^5	σ_{N_2} (Å)	3.798
γ_a (A/m^2)	1.344 x 10^{10}	σ_{O_2} (Å)	3.467
γ_c (A/m^2)	2.051 x 10^9	ε_{H_2}	59.7
l_a (μm)	750	ε_{H_2O}	809.1
l_c (μm)	50	ε_{N_2}	71.4
ξ (μm)	5.4	ε_{O_2}	106.7
n	0.48		

4.2.2 Calculation Procedure

The calculation begins with defining the desired values of fuel utilization of SOFC including operating voltage, temperature, and parameters of anode and cathode inlet flow rate in each gas component. Fuel utilization was divided into many small regions with step size of 0.01 in SOFC stack to calculate the current density and area in each region as illustrated in Figure 4.2.

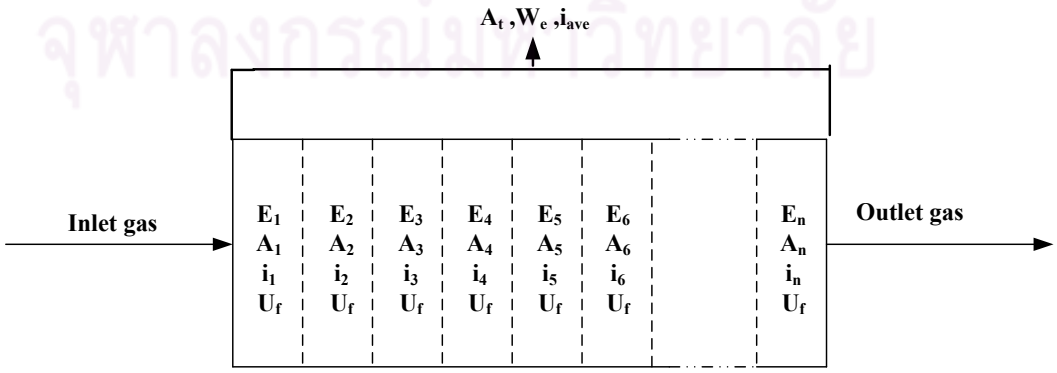

Figure 4.2 The schematic SOFC module for numerical calculation

The sets of equation in Section 4.2.1 are arranged and placed on the potential balance in Eq. (4.12). A constant operating voltage (V) is defined and open circuit voltage (E) is early computed. Thereafter, the current density in each region is obtained by calculating with trial and error until the difference between E and the total polarizations is equal to the operating voltage (V) on Eq. (4.12). The small element of SOFC area can be calculated by the following equation:

$$A_f = \frac{2F(\Delta U_f)}{i_f} \tag{4.31}$$

The numerical calculation is continued until the value of U_f reaches the desired fuel utilization. The total SOFC area (A_{total}) can be obtained by summation of each small area (A_f). Then, the average current density (i_{ave}), power density (p_{ave}) and total electrical power (W_{e}) are calculated with Eqs. (4.32), (4.33) and (4.34), respectively.

$$i_{ave} = \frac{2F(U_f)}{A_{total}} \tag{4.32}$$

$$p_{ave} = i_{ave}V \tag{4.33}$$

$$W_e = p_{ave}A_{total} \tag{4.34}$$

The computational algorithm for determining SOFC performance is expressed as Figure 4.3.

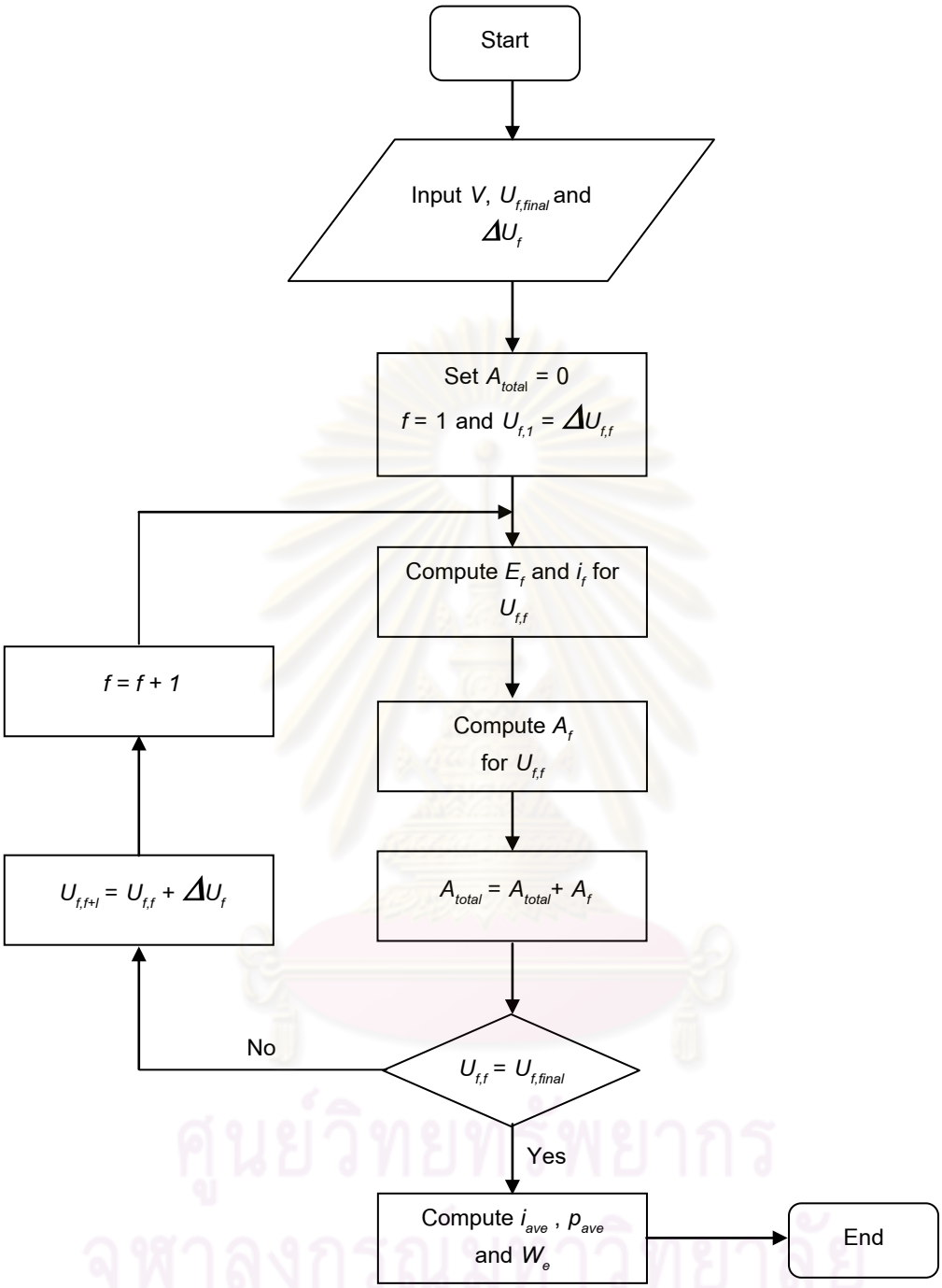

Figure 4.3 The flow chart of algorithm for computation of a fuel cell

4.3 SOFC system configurations

The process of SOFC system fuelled by bioethanol fundamentally consisted of preheaters, reformer, SOFC, and afterburner. In this research, the extra bioethanol pretreatment unit is further installed into this system as schematically shown in Figure

4.4. Bioethanol solution of 10wt% or 4.16mol% is introduced into a pretreatment unit operated under 348 K to carry out a desired ethanol concentration of 25 mol%, a stoichiometric ratio for ethanol steam reforming reaction in Eq. (2.7).

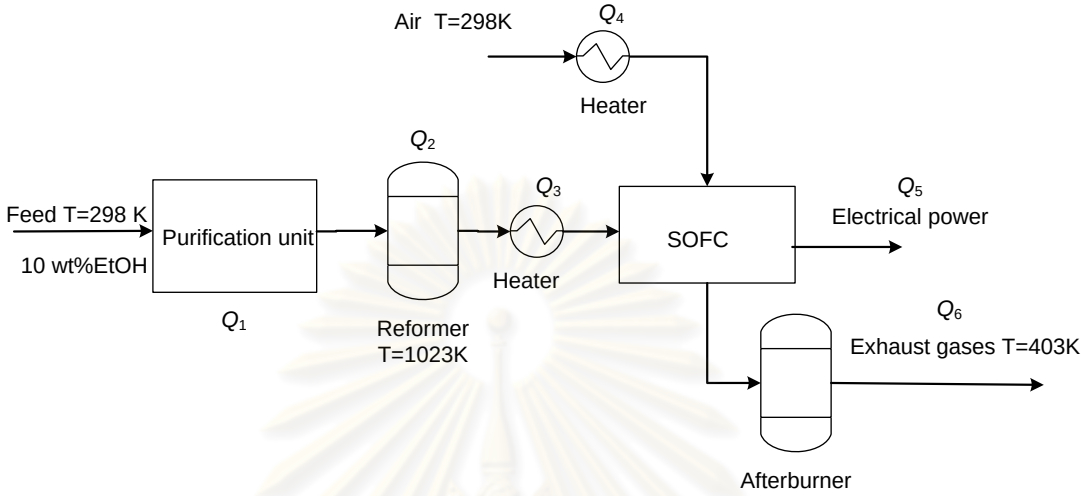

Figure 4.4 Schematic diagram of bioethanol-fuelled SOFC system

Afterwards, the stream with 25 mol% ethanol is fed into an external reformer operated at 1023 K under thermodynamic equilibrium condition. Ethanol steam reforming reaction is considered as a main reaction for producing hydrogen rich gas and the reactions in Eqs. (2.8) and (2.9) are defined as undesired reactions occurring simultaneously with the main reaction including water gas shift reaction as shown in Eq. (2.22). These reactions are assumed to take place isothermally in an external reformer simulated by Aspen plus. The reformed hydrogen rich gases are fed into an ER-SOFC to produce electrical power at the anode chamber whilst excess air (5 times) is preheated and fed into the cathode chamber. Exhausted gases released from an SOFC containing unreacted fuels are brought into the afterburner to combust and recover heat from this residue to supply energy to the other heat-demanding units i.e. purification unit, reformer, and preheaters. From Figure 4.4, the heat obtained from SOFC and the afterburner represented as Q_5 and Q_6 are assigned to have a role for supplying thermal energy to the heat-demanding units represented in Q_1, Q_2, Q_3 and Q_4. The final temperature of exhausted gases vented to the environment is specified at 403 K. In some cases, the overall performance of SOFC system is evaluated under the condition of no external energy demand or $Q_{net} = 0$ calculated by conventional energy balance as below:

$$Q_{net} = Q_5+Q_6-Q_1-Q_2-Q_3-Q_4 = 0 \qquad (4.35)$$

and the definition of overall electrical efficiency of this system is given by:

$$\eta_{elec,ov} = \frac{W_{e,net}}{mol_{EtOH} . LHV_{EtOH} + External\ \ Heat\ \ Demand} \qquad (4.36)$$

where $W_{e,net}$ is the net electrical energy gained from the system after subtracting power consumption of vacuum pump. LHV_{EtOH} is the lower heating value of bioethanol feed. According to Eq. (4.35), when $Q_{net} < 0$, the SOFC system requires additional thermal energy from an external source and these amounts of heat are taken into account as external heat demand term in Eq. (4.36) of overall electrical efficiency.

CHAPTER V

RESULTS AND DISCUSSIONS

5.1 Effect of pervaporation membrane type on performance of SOFC system

In this section, the performance of SOFC system using pervaporation with two different membrane types, namely hydrophilic and hydrophobic membranes has been investigated as depicted in Figure 5.1. In principle, although bioethanol as a dilute ethanol solution was suitable for hydrophobic type due to lower energy consumption for a small amount of ethanol removal, this membrane type was inevitable to face the limitation of low ethanol separation factors as shown in Figure 5.1. It may perform a low ethanol recovery or obtain ethanol concentration below the target level (25 mol% ethanol). On the contrary, a hydrophilic type may assist to reach the desired ethanol concentration owing to high water separation factors, although it requires high energy supply to remove plenty of steam. Therefore, it is necessary to compare the performance between hydrophilic and hydrophobic membrane for pervaporation and their effects on the overall SOFC system performance.

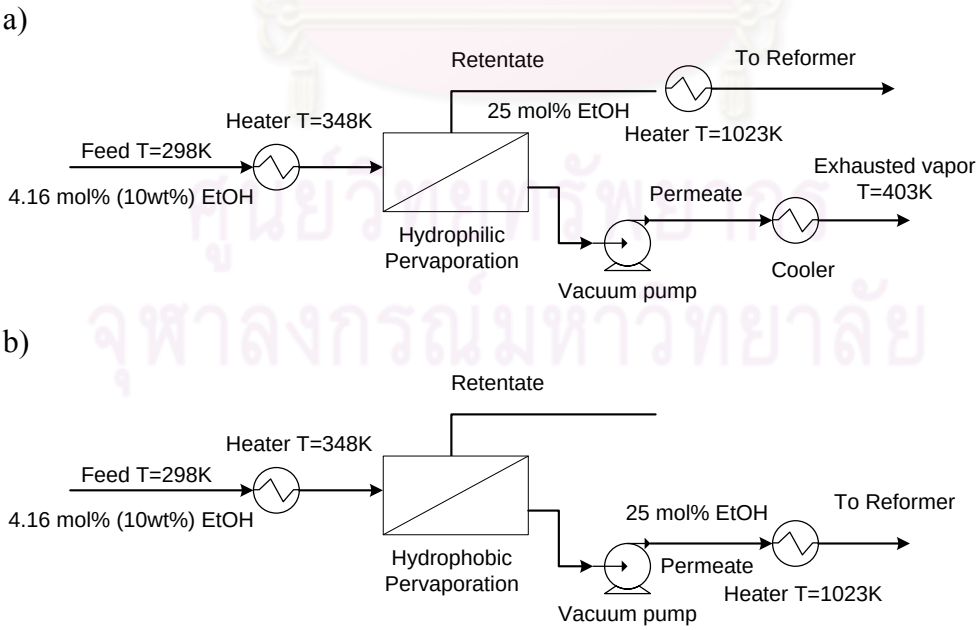

Figure 5.1 Pervaporation membrane type configurations: a) Hydrophilic and b) Hydrophobic

According to Figure 5.1, for case a), a hydrophilic pervaporation was used to remove excess water from the feed by permeating through a membrane until the retentate side of the pervaporation contained 75 mol% water. The heat accumulated in steam on the permeate side was recovered to supply the heater operated at 1023K until its exhausted temperature reached 403 K to redeem a high thermal energy consumption in this case. When considering case b), ethanol was permeated by hydrophobic pervaporation to obtain a permeate stream of 25 mol% ethanol.

Table 5.1 A review of separation performance with different membrane types of pervaporation unit

Hydrophobic membrane				
Membrane material	Ethanol in feed (wt%)	Temperature (K)	Separation factor ($\alpha_{E/W}$)	Reference
Silicalite-1/α-Al_2O_3	5	348	78	Lin et al. (2001)
Silicalite-1/Mullite	10	333	72	Lin et al. (2000)
PDMS	10	348	6.25	Baker et al. (2010)
PTMSP(-silica)	10	348	10.7	Gonzalez-Velasco et al. (2003)
PDMS(ZSM-5 mixed matrix)	10	348	15.5	Baker et al. (2010)
ZSM-5/α-Al_2O_3	10	348	24	Kita (1998)
Hydrophilic membrane				
Membrane material	Water in feed (wt.%)	Temperature (K)	Separation factor ($\alpha_{W/E}$)	Reference
Zeolite NaA, disk	90	303	>10000	Kumakiri et al. (1999)
Cellulose ester	90	348	0.76	Baker et al. (2010)
NaA, Mullite/Al_2O_3	10	348	42000	Kondo et al. (1997)

5.1.1 Separation characteristics of hydrophilic and hydrophobic membranes

Figure 5.2 presents the values of required separation factor in order to purify dilute bioethanol to 25 mol%ethanol at any specified ethanol recovery (*R*%). It was found that the required separation factor increased following by increasing ethanol recovery especially at high ethanol recovery. In addition, Figure 5.2 also expresses the corresponding permeate flow rates in each membrane type. For the hydrophobic type, the desired ethanol product is at the permeate stream while for the hydrophilic type the ethanol product is at the retentate stream. The results show that when using the hydrophilic membrane a large amount of water are needed to be removed to the permeate side (more than 240 kmol/s) to obtain a desired ethanol composition in the retentate stream, in contrast to a hydrophobic type, much smaller amount of its permeate flow rates are required to achieve a desired ethanol removal. Different amount of permeate flow rates obtained in each membrane type can convey to the required energy including electrical power of vacuum pump and total thermal energy at different ethanol recovery as illustrated in Figures 5.3a) and 5.3b) for hydrophilic and hydrophobic types, respectively. It can be seen that both total thermal energy and power of vacuum pump increase consistently when increasing an ethanol recovery.

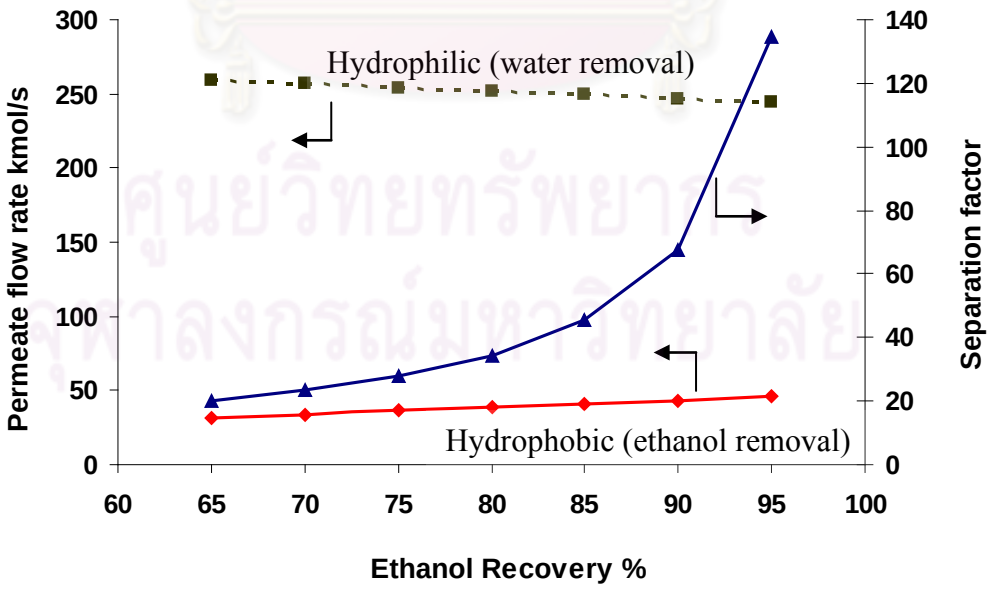

Figure 5.2 Effect of ethanol recovery on the separation factor and flow rates.

a)

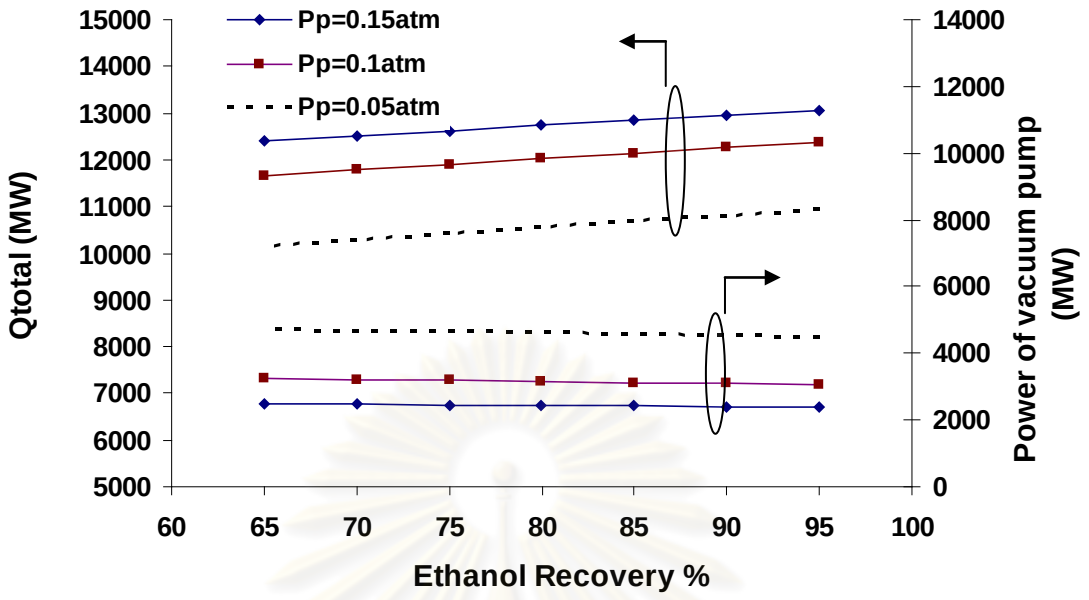

b)

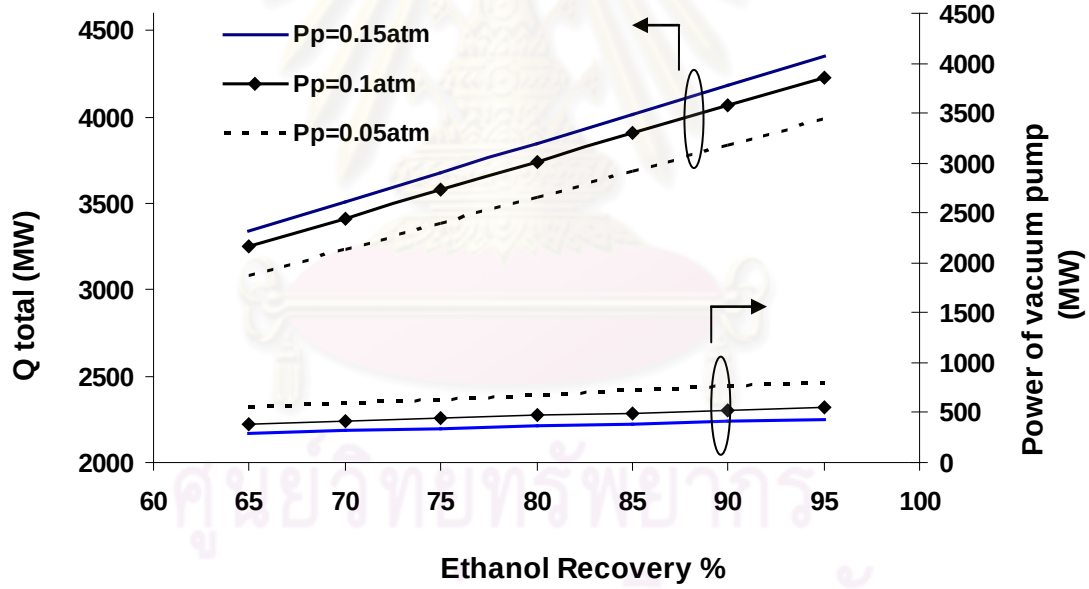

Figure 5. 3 Effect of e thanol recovery on the total t hermal e nergy a nd pow er of vacuum pump consumption for: a) hydrophilic and b) hydrophobic membranes.

When c omparing b etween t wo membrane t ypes, it is apparent that t he hydrophilic type in Figure 5.3a) uses about 3-4 times of thermal energy higher than that of the hydrophobic type shown in Figure 5.3b) because it requires plenty of heat for vaporizing a large amount of water as indicated in Figure 5.2. It also utilizes more power at the vacuum pump according to the same reason. From Figure 5.3, there is an

inverse relationship between total thermal energy and power of vacuum pump. When the permeate pressure was reduced, the vacuum pump consumed more electrical power and the permeate temperature became higher as represented by Eq. (4.6).
Due to the higher permeate temperature, it can reduce burden of heater located prior to the reformer required to heat up to 1023 K so the total thermal energy becomes lower. Although the hydrophobic type required energy much less than the hydrophilic type, the separation factor values obtained in Figure 5.2 available for the hydrophobic type can serve only at low ethanol recovery ranges while these from the hydrophilic type can be available even at high ethanol recovery as shown in Table 5.1.

5.1.2 Performance assessment of SOFC system using pervaporation with two different membrane types

After discovering the characteristic results of both membrane types from the previous studies, evaluation of overall performance of SOFC system using both membrane types based on the net energy were performed and the results are shown in Figure 5.4. It is found that an increase of fuel utilization brought about the decrease of net energy in all cases.

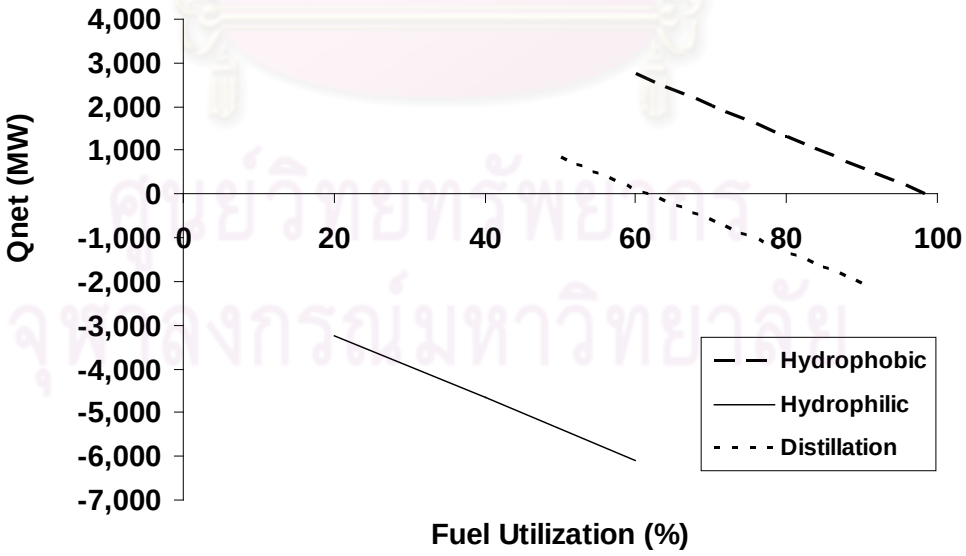

Figure 5.4 Effect of fuel utilization on the net energy (Q_{net}) of SOFC system with two different membrane types of pervaporation and distillation column (R_{EtOH} = 85%, V = 0.6V, T_{SOFC} = 1073K, P_p = 0.15atm).

The low operating voltage of 0.6V is specified in order to have some fuel utilization values which assist the system especially hydrophilic case to be operated at least $Q_{net} = 0$. At this condition, the external heat sources are not required but the results indicate that it is impossible to operate the SOFC system with hydrophilic pervaporation at this condition. A distillation column is considered as having poorer performance than a pervaporation which is then compared with the other two membrane types (Figure 5.4) to demonstrate that it can be operated below $Q_{net} = 0$ and offers its performance superior to hydrophilic membrane type. Therefore, a hydrophobic type still becomes a suitable alternative for purifying bioethanol regarding a lower energy consumption.

5.1.3 Performance characteristics of SOFC system integrated with hydrophobic pervaporation

According to the previous studies, the use of hydrophobic pervaporation with the SOFC system can be operated without external energy demand. The operating conditions of hydrophobic pervaporation are further investigated to show the performance characteristics of the overall system based on $Q_{net} = 0$.

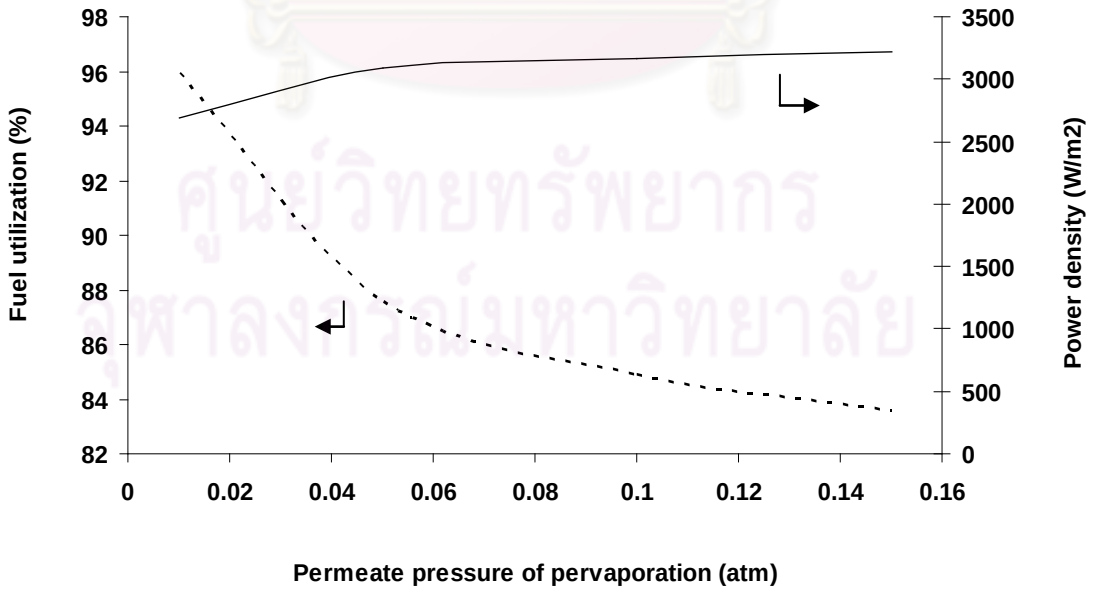

Figure 5.5 Effect of permeate pressure of pervaporation on fuel utilization and power density of SOFC system based on $Q_{net} = 0$ (R_{EtOH} = 80%, V = 0.7V, T_{SOFC} = 1073K).

Since a pervaporation unit required electrical power to operate a vacuum pump apart from its thermal energy requirement, the effect of operating permeate pressure on SOFC system needs to be studied. Figure 5.5 shows the results of fuel utilization and power density of SOFC at different permeate pressure values. When a vacuum pump operates at lower permeate pressures, it consumes more electrical power to support its conditions, but the temperature of permeate stream becomes higher. It can reduce burden of a heater located prior to the reformer operated at 1023 K because of higher heat accumulated in the permeate stream. Consequently, SOFC system operated under $Q_{net} = 0$ must consume more fuel for converting into electricity as represented with increasing a fuel utilization especially at low permeate pressure on Figure 5.5. This reduces an amount of the remaining fuel being combusted in the afterburner that releases excess heat, while the power density shows a little effect from decreasing the permeate pressures as the operating voltage was assumed constant at 0.7 V. Regarding the effect of permeate pressure on the overall electrical efficiency, an electrical power consumption of a vacuum pump takes quite no effect in deceasing of the electrical efficiency. It was found that the overall electrical efficiencies from the specified permeate pressure range were obtained at rather the same of 39.36%.

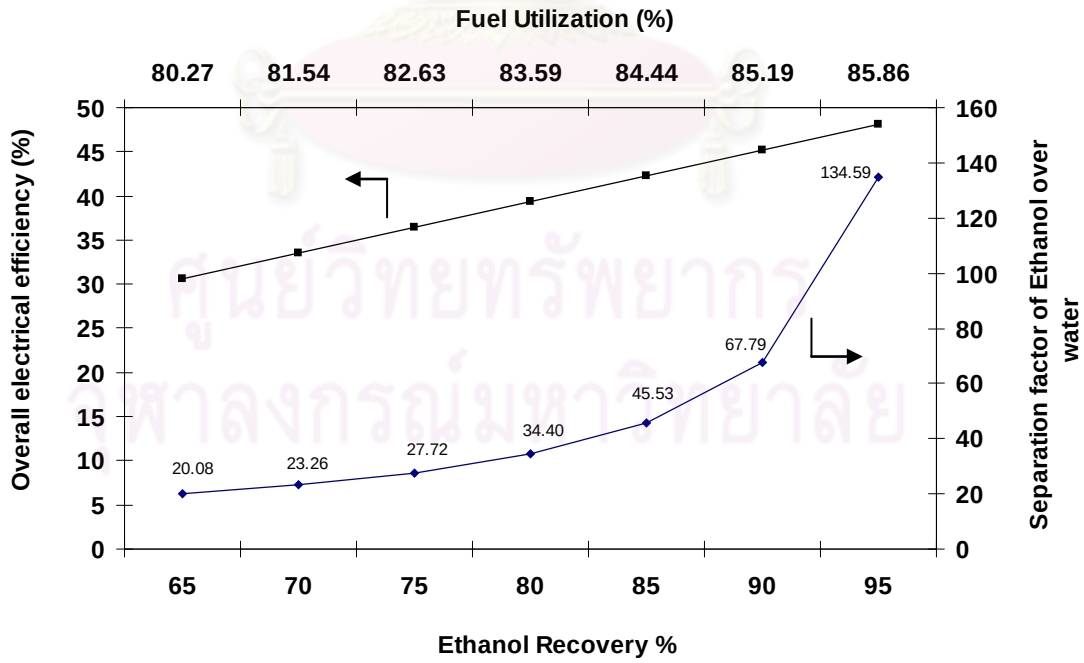

Figure 5. 6 Effect of ethanol recovery on the overall electrical efficiency of SOFC system and acquired separation factor using hydrophobic pervaporation based on $Q_{net} = 0$ ($V = 0.7$V, $T_{SOFC} = 1073$K, $P_p = 0.15$atm).

Figure 5.6 shows the performance of SOFC system including the overall electrical efficiency, fuel utilization and $\alpha_{EtOH/Water}$ at different values of ethanol recovery. The results indicate that when increasing the ethanol recovery, it certainly requires a membrane with much higher ethanol separation factor particularly in the range of 85-95% ethanol recovery, but the system can achieve a higher overall electrical efficiency. At the ethanol recovery of 95%, the system can gain the overall electrical efficiency of almost 50%, although it requires an ethanol separation factor as high as 134.59 and the system also consumes more fuel as described by increasing the fuel utilization values in Figure 5.6. In fact, a hydrophobic membrane which has a high ethanol separation factor to serve this desired ethanol concentration with high ethanol recovery is not available. It is necessary to have other techniques to solve this problem or further assist the separation performance of the hydrophobic membrane.

5.2 Performance improvement of SOFC system with hybrid vapor permeation-pervaporation process

In this section, a pervaporation based on available membrane materials from Table 5.1 is considered as a purification unit for SOFC system fuelled by bioethanol to represent more realistic results. In the first part, the separation efficiency of pervaporation in each membrane material is compared at various values of ethanol recovery. Thereafter, the separation performance is further improved by introducing a vapor permeation installed after the pervaporation to gain a desired ethanol concentration at a higher ethanol recovery. To serve this propose, a selection of appropriate membrane type for vapor permeation is further investigated by considering the membrane availability and optimal overall efficiency.

a)

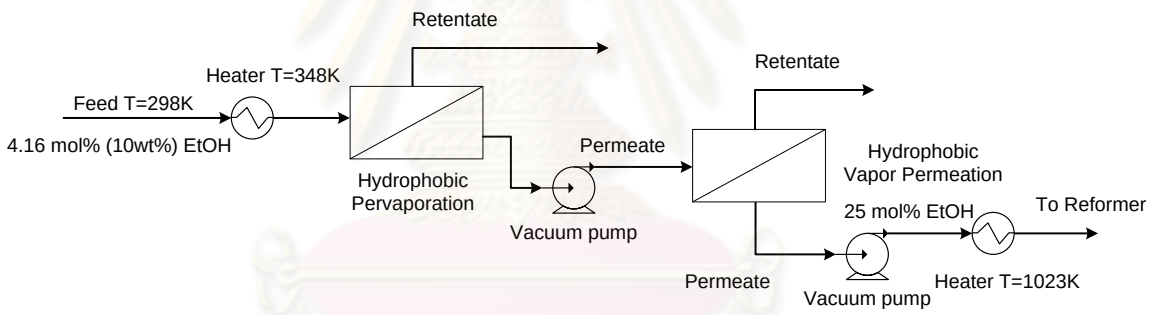

b)

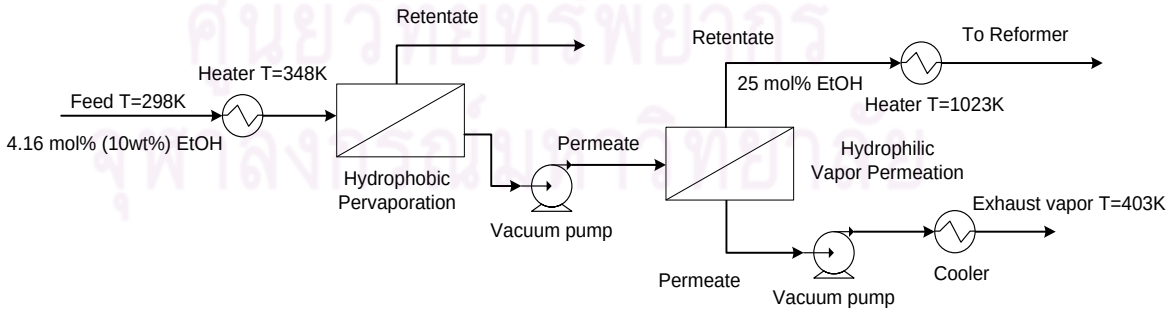

Figure 5. 7 Purification process configurations: a) pervaporation with hydrophobic vapor permeation b) pervaporation with hydrophilic vapor permeation

For the SOFC system configurations, various bioethanol purification processes were considered as depicted in Figure 5.7. The pervaporation with hydrophobic vapor permeation and pervaporation with hydrophilic vapor permeation were placed on a) and b), respectively. A hydrophobic membrane was chosen for the pervaporation unit in accordance with the principle mentioned before. Ethanol recovery (R_{EtOH}) of vapor permeation in cases b) and c) were defined at 99%. To consume less electrical power, the vacuum pumps of both pervaporation and vapor permeation were assumed to be operated at 0.15 atm which was feasible in practical operation.

For case a), the hydrophobic vapor permeation was installed after the pervaporation to obtain a permeate stream of 25 mol% ethanol at a higher ethanol recovery. On the other hand, the hydrophilic vapor permeation in case b) was used to remove excess steam permeating through the membrane until the retentate side of the vapor permeation contained 75 mol% water. It was assumed that the heat available in the permeate stream could be recovered until its exhaust temperature reached 403 K (Wassana Jamsak et al., 2007).

5.2.1 Effects of ethanol recovery and membrane material on the obtained ethanol concentration in hydrophobic pervaporation

A separation performance of hydrophobic pervaporation is assessed based on the performance of real membrane materials as summarized in Table 5.1. The selected membranes are PDMS, PTMSP, PDMS (ZSM-5 mixed matrix) and ZSM-5 (α-Al_2O_3) which offer the ethanol separation factor values of 6.25, 10.7, 15.5, 24, respectively. The results illustrate that when increasing the ethanol recovery of pervaporation, the obtained ethanol concentrations from all membranes are declined as illustrated in Figure 5.8. For the membranes with low ethanol separation factor such as PDMS with $\alpha_{E/W}$ = 6.25, the desired ethanol concentration (25 mol%) cannot be achieved at any ethanol recovery even at low recovery values. When consider of the other three membranes, PTMSP membrane with the ethanol separation factor of 10.7, just a little higher than that of PDMS, merely obtains 25 mol% ethanol at 31.16% ethanol recovery. For PDMS(ZSM-5 mixed matrix) and ZSM-5(α-Al_2O_3) membranes, they can provide 25mol%ethanol with more than 50% ethanol recovery (54% and 71%, respectively). At high ethanol recovery such as 95%, Figure 5.8 shows that there is no

significant difference in the obtained ethanol concentration among all membranes regardless of membrane separation factor values. As a result of increasing the ethanol recovery, a high ethanol separation factor value for hydrophobic pervaporation should be required to achieve the desired ethanol concentration with high ethanol recovery.

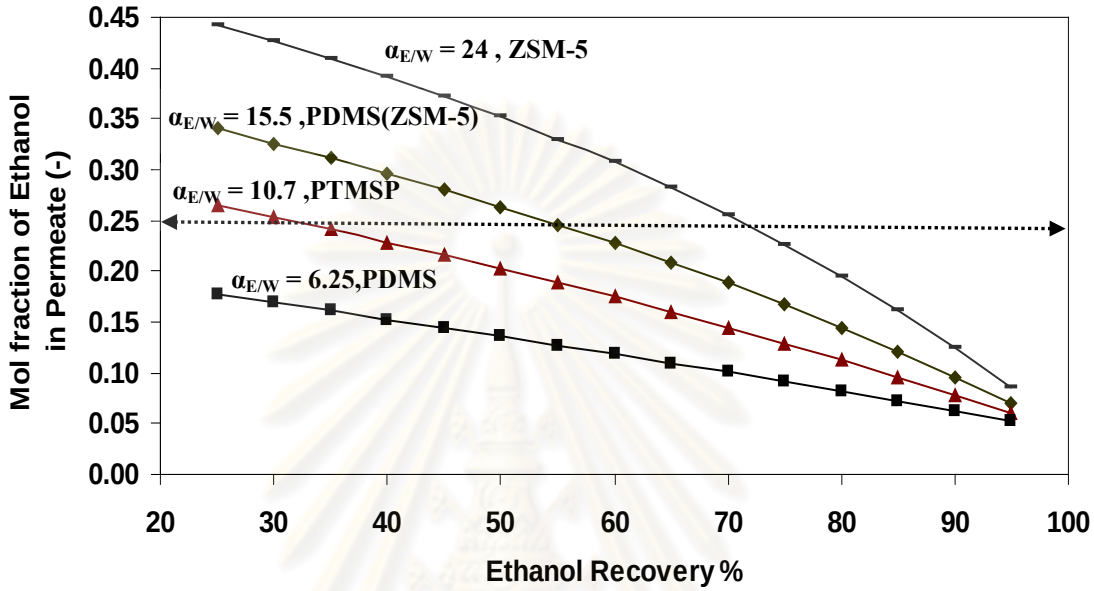

Figure 5.8 Effect of ethanol recovery with various membrane materials on ethanol concentration using hydrophobic pervaporation.

5.2.2 Performance comparison between different vapor permeation membrane types

According to the previous results in Figure 5.8, it is clear that due to the low sepration factor of the hydrophobic membrane for pervaporation, the desired ethanol concentration of 25% can only be achieved with some membrane materials but the obtained ethanol recovery is still low. To improve its poor separation performance, a vapor permeation installed after the pervaporation is proposed. The effect of membrane types (hydrophobic and hydrophilic) is investigated. PTMSP membrane having the lowest ethanol recovery at the desired ethanol concentration which was regarded as the worst case is considered to be a reference case study in this section in order to clearly demonstrate its performance improvement.

5.2.2.1 Effect of pervaporation ethanol recovery on the required vapor permeation separation factor and permeate flow rate

Figure 5.9 shows the permeate flow rates of the hydrophobic and hydrophilic vapor permeations at different values of pervaporation ethanol recovery of PTMSP ($\alpha_{E/W}$ =10.7)-based membrane. The ethanol recovery in a vapor permeation was specified at 99%. It can be observed that the permeate flow rates of the hydrophobic type increase gradually when increasing the pervaporation ethanol recovery. However, for the hydrophilic type whose desired ethanol composition of 25mol% appears at the retentate stream, the permeate flow rate increases rapidly with increasing the pervaporation ethanol recovery. At the low range of pervaporation ethanol recovery, the values are smaller than those of the hydrophobic membrane but the opposite trend is observed at higher ranges of pervaporation ethanol recovery. The upper x-axis of Figure 5.9 showed the obtained ethanol mol fraction in the permeate stream of the pervaporation. The values decline from the desired ethanol concentration when increasing the ethanol recovery to above 31.16%. The right y-axis of Figure 5.9 indicates that it requires a higher membrane separation factor for the vapor permeation when increasing the pervaporation ethanol recovery.

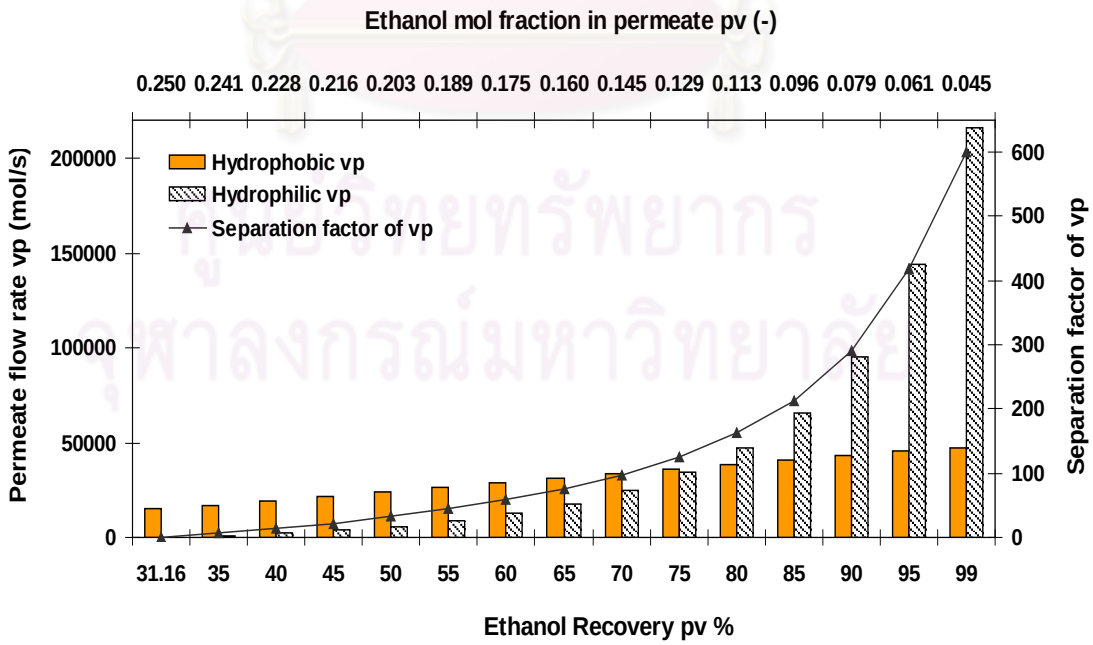

Figure 5.9 Effect of ethanol recovery of PTMSP pervaporation on permeate flow rate between two types and separation factor of vapor permeation.

The value of the vapor permeation separation factor increases above 100 at the ethanol recovery greater than 70%. At a higher range of ethanol recovery (80-99%), both cases require much higher separation factor to achieve their conditions. Based on the principle stated by Wijmans and Baker (1995), they claimed that the permeability data of pervaporation can be applied as a preliminary estimation for vapor permeation. Therefore, from the results shown in Figure 5.9, it indicates that the required ethanol separation factor values for hydrophobic type are not available in commercial membranes. On the contrary, the obtained water separation factor of hydrophilic vapor permeation is available in real membranes according to the high $\alpha_{W/E}$ (Table 5.1).

5.2.2.2 Effect of pervaporation ethanol recovery on energy consumption within vapor permeation

The results of energy requirement including thermal and electrical energy were presented in Figure 5.10. Three SOFC systems (i.e. pervaporation alone, pervaporation with hydrophobic vapor permeation and pervaporation with hydrophilic vapor permeation) were considered.

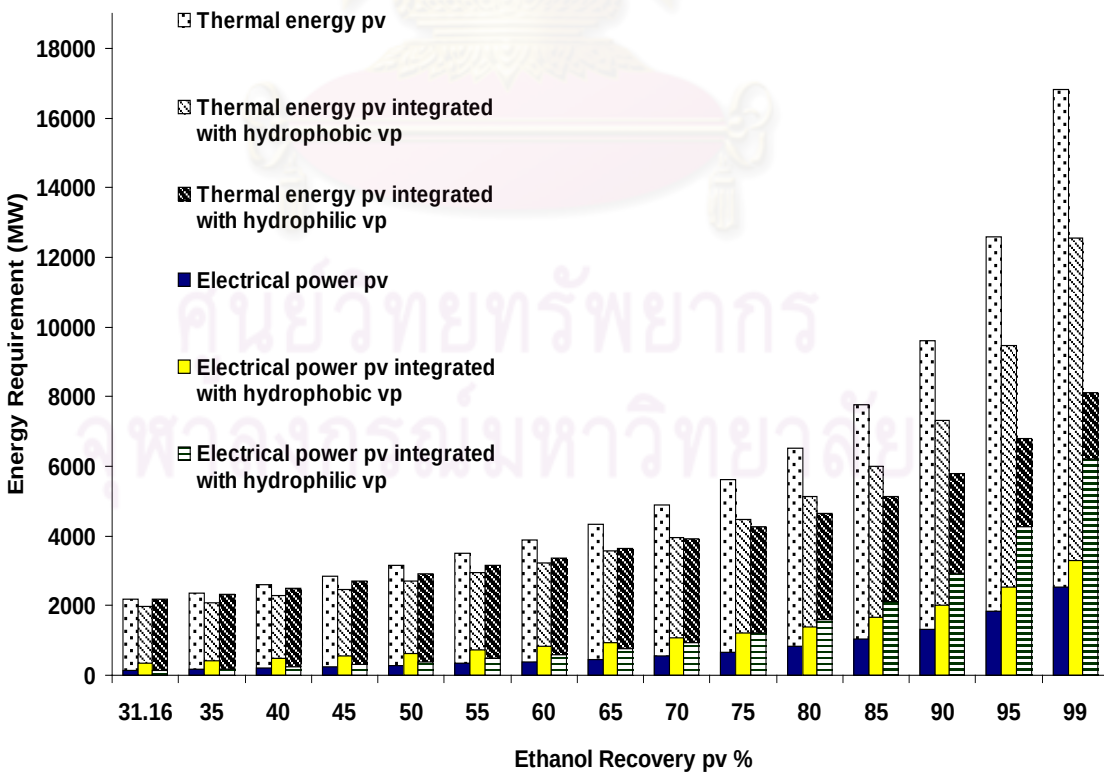

Figure 5. 10 Effect of ethanol recovery of PTMSP pervaporation on energy requirement of both types of vapor permeation

For hydrophobic pervaporation, the demand of thermal energy is the highest compared to the other two cases especially at high ethanol recovery but it requires the lowest electrical power. When the other two cases are considered at the low range of ethanol recovery, an integration with the hydrophilic vapor permeation consumes thermal energy a little higher than in the other case. Nevertheless, when the ethanol recovery is further increased, the demand of thermal energy does not significantly increase and it becomes lower than that of the hydrophobic vapor permeation at 70% ethanol recovery. Although the hydrophilic vapor permeation requires less thermal energy, it consumes higher electrical power.

5.2.3 Performance evaluation of SOFC system under appropriate operating conditions

5.2.3.1 Effects of SOFC operating voltage and fuel utilization on the net thermal energy (Q_{net})

From the above studies, the proposed purification process could offer the desired ethanol concentration at higher ethanol recovery by using integrated pervaporation and vapor permeation. A pervaporation with poor ethanol separation factor recovered a high amount of ethanol but the ethanol concentration was still lower than the desired concentration. Then, the permeate stream was purified by vapor permeation to reach 25 mol% of ethanol. However, an electrical power consumption was required further from a vacuum pump of vapor permeation as shown in Figure 5.10. Therefore, in this section, it is necessary to evaluate the overall performance focusing on the net thermal energy (Q_{net}) obtained from the SOFC systems integrated with the proposed purification process. The effects of fuel utilization (U_f) and operating voltage (V) on Q_{net} are presented in Figures 5.11 and 5.12 for high and low ranges of ethanol recovery for both types of vapor permeation, respectively. At high ethanol recovery, Figure 5.11a) referring to the hydrophobic type shows that there is a narrow range of fuel utilization values which can be operated above Q_{net}=0, while Figure 5.11b) referring to the hydrophilic type shows a wider range of fuel utilization values. This means the condition has the remaining heat higher than the other case at the same fuel utilization and operating voltage. At low ethanol recovery, Figures 5.12a) and 5.12b) show slightly different net thermal energy between the hydrophobic and hydrophilic

types, indicating that the hydrophilic vapor permeation provides the net thermal energy slightly lower than the hydrophobic vapor permeation. However, this section only investigates the feasibility of operating conditions that can serve $Q_{net} \geq 0$. An electrical efficiency is another important performance indicator of the system to be evaluated further in the next section.

a)

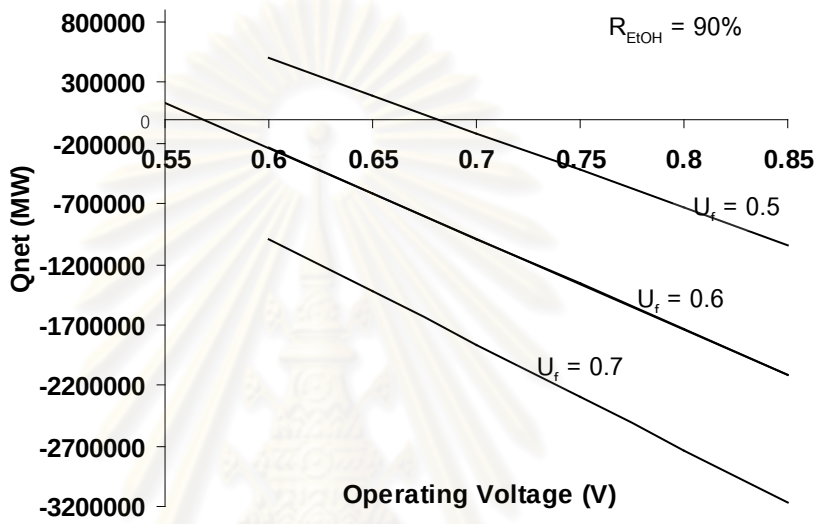

b)

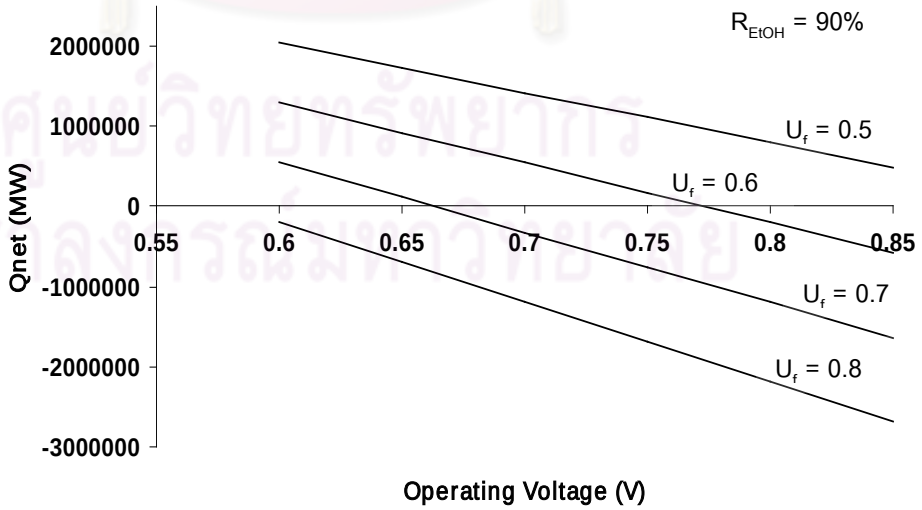

Figure 5.11 Effects of operating voltage and fuel utilization on Q_{net} at high ethanol recovery: a) hydrophobic vapor permeation and b) hydrophilic vapor permeation.

a)

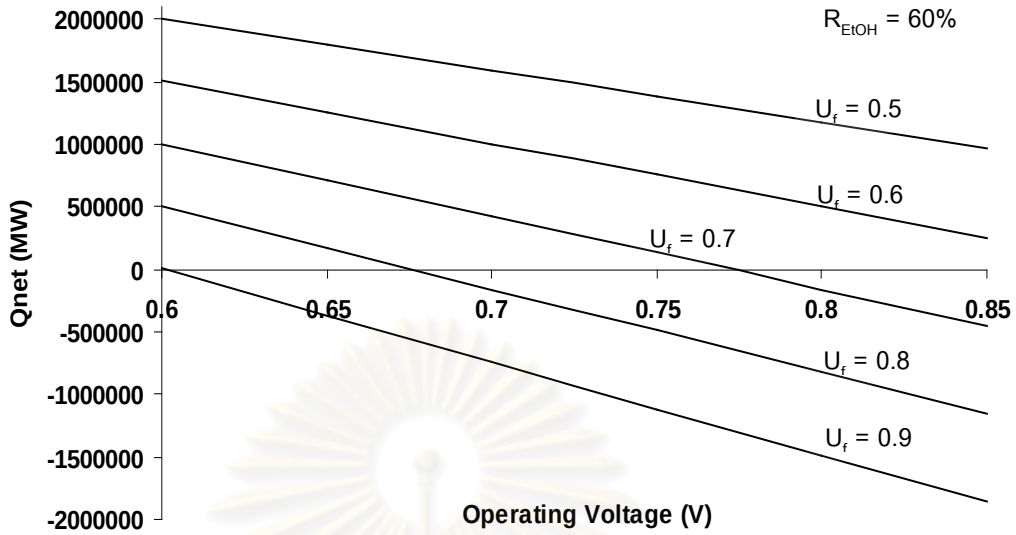

b)

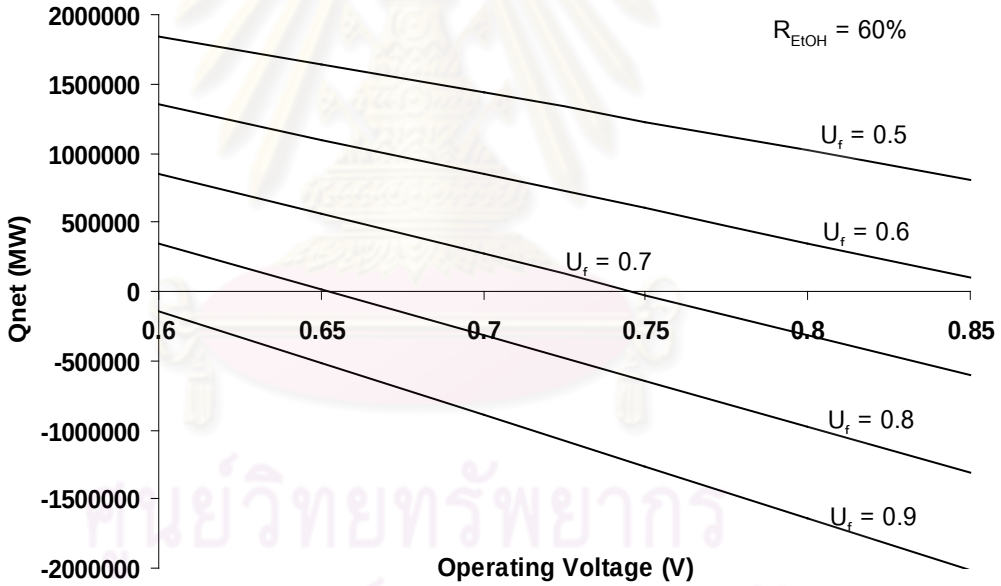

Figure 5.12 Effects of operating voltage and fuel utilization on Q_{net} at low ethanol recovery: a) hydrophobic vapor permeation and b) hydrophilic vapor permeation.

5.2.3.2 Optimal efficiency comparison between SOFC systems with two different membrane types of vapor permeation at the condition of Q_{net} = 0

In order to operate the SOFC without demanding additional energy from an external source and to achieve the highest electrical efficiency, the system should be

operated at the condition with net thermal energy (Q_{net}) equals to zero. From the previous section, it was feasible to operate an SOFC system with the proposed purification process under this condition. In this section, the electrical efficiency comparison between the SOFC systems with hydrophobic and hydrophilic vapor permeation is studied at various values of pervaporation ethanol recovery to determine a suitable purification system for operation. From Figure 5.13, the results obtained from simulation studies are based on the following operating conditions: Operating voltage = 0.6 V and T_{SOFC} = 1073 K. It should be noted that the SOFC stack can be operated at other values of operating voltage; however, based on the energy self-sufficient condition in this work, the overall electrical efficiency does not vary with the operating voltage. At higher operating voltage, although the SOFC stack efficiency is higher, the lower fuel utilization is required in order to leave sufficient fuel for generating enough heat at the afterburner for use within the system. The overall electrical efficiency gradually increases when increasing the ethanol recovery up to 75%. At higher ethanol recovery, the energy requirement including thermal and electrical energy for purification system rapidly increases as shown in Figure 5.10. Accordingly, the overall electrical efficiency drops dramatically especially in case of the hydrophobic type represented by the dashed line.

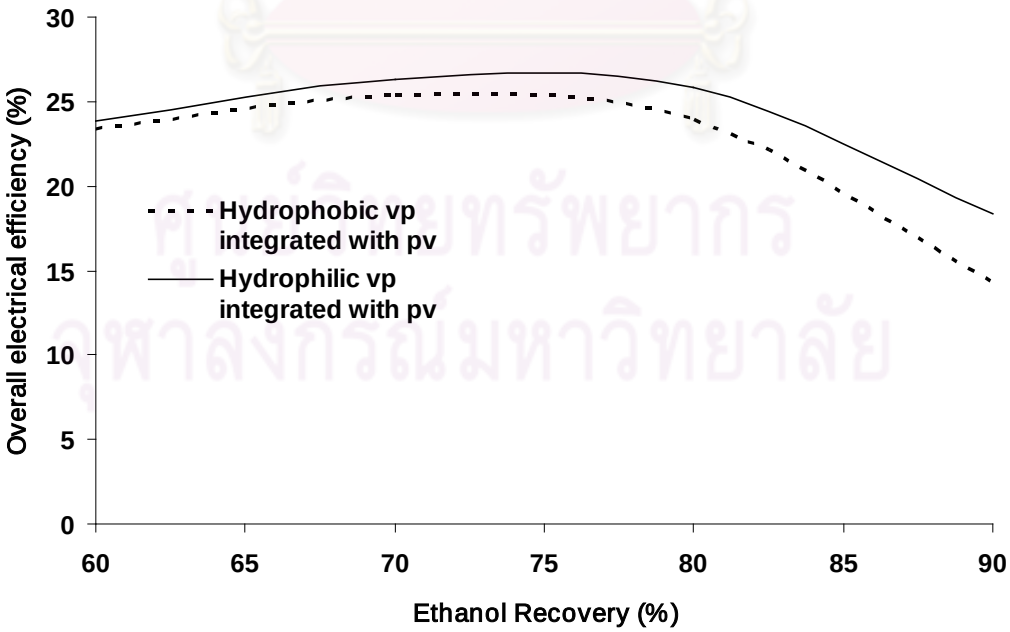

Figure 5.13 Effect of ethanol recovery on the overall electrical efficiency of two different membrane types of vapor permeation.

The system with hydrophobic type offers the overall system efficiency lower than that with the hydrophilic type because its summation of energy consumption including thermal and electrical energy is higher than that of the hydrophilic type especially at high ethanol recovery as illustrated in Figure 5.10. As shown in Figure 5.13, it was found that the optimal overall electrical efficiency obtained from the hydrophilic type was 26.56% at 75% ethanol recovery.

5.2.3.3 Efficiency comparison of SOFC systems before and after installing a vapor permeation unit

After a suitable purification system was obtained from the previous studies, the overall electrical efficiencies for the SOFC systems with and without vapor permeation are compared in this section based on the following operating conditions: Operating voltage = 0.6 V and T_{SOFC} = 1073 K. According to the use of PTMSP pervaporation with $\alpha_{E/W}$ = 10.7 as a base case, Table 5.2 shows the results when installing the hydrophilic vapor permeation which was a suitable choice to be installed after the pervaporation. The obtained electrical efficiency is 26.56% compared to 10.96% of the SOFC with a pervaporation alone because it can recover an amount of ethanol at 75% while the base case can only recover ethanol at 31.16% for 25 mol% ethanol concentration. Although an additional vapor permeation requires an electrical power for operating the vacuum pump, it still obtains the net electrical power ($W_{e,net}$) higher than the case with a single pervaporation because of no heat consumption requirement in a separation of vapor permeation as mentioned earlier and the extra electrical power consumption takes only a little effect on the overall efficiency. Therefore, the system does not significantly reduce the fuel utilization values. Moreover, it can be observed that the addition of vapor permeation system has the overall electrical efficiency which can overcome the case of PDMS(ZSM-5 mixed matrix) with $\alpha_{E/W}$ = 15.5. Nevertheless, it should require higher ethanol separation factor values of hydrophobic pevaporation for a desired ethanol concentration at high ethanol recovery in order to gain higher overall system efficiency as seen in the case of ZSM-5/α-Al_2O_3 which shows the electrical efficiency of 34.02%.

Table 5.2 Efficiency comparison of SOFC system between with and without extra vapor permeation

Membrane Pervaporation	Ethanol Recovery (%) (25mol%ethanol)	Fuel Utilization (%)	$W_{e,net}$ (MW)	Efficiency (%)
PTMSP ($\alpha_{E/W}$ =10.7)	31.16	67.75	1,765.7	10.96
PTMSP ($\alpha_{E/W}$ = 10.7) with hydrophilic vapor permeation ($\alpha_{W/E}$ = 125.2)	75	86.5	5,392.3	26.56
PDMS(ZSM-5mixed matrix) ($\alpha_{E/W}$ = 15.5)	54	89.2	4,007.5	23.96
ZSM-5/α-Al_2O_3 ($\alpha_{E/W}$ = 24)	71	95.3	5,666.25	34.02

5.3 Performance comparison of SOFC system integrated with different bioethanol purification processes

From the above studies, a hybrid vapor permeation-pervaporation process was proven as an efficient separation performance brought to obtain higher performance of SOFC system following by the results on Table 5.2. To obviously show its performance improvement, the overall electrical efficiency of SOFC system using conventional distillation column and hybrid vapor permeation-pervaporation process should be compared. From Table 5.2, a hydrophobic pervaporation membrane of ZSM-5/α-Al_2O_3 which has the highest separation factor ($\alpha_{E/W}$ = 24) is further developed by sequentially adding a hydrophilic vapor permeation and the results of its system configurations are shown in Figure 5.14. Based on the operating conditions: Operating voltage = 0.75V, T_{SOFC} = 1073K and Permeate pressure = 0.15atm, it can be observed that an increase of ethanol recovery from 71% to 75% shows a significant improvement of the overall electrical efficiency from 34.28% to 45.45%. When increasing the ethanol recovery above 75%, the remaining thermal energy represented

by Q_{net} on the right y-axis is released from the system eventhough the fuel cell is operated at almost highest fuel utilization (U_F = 99%) to produce high electricity and reduce the residual fuel for combustion. It can be explained that the extra added vapor permeation required no thermal energy for its separation but consumed some electrical power for operating the vacuum pump, while the amount of ethanol considered as a fuel can be obtained even more. Accordingly, heat and electrical power requirement of the system can be enough supplied by SOFC without relying on the afterburner to combust residual fuel to generate excess heat released to the environment. Since the vacuum pumps of both pervaporation and vapor permeation consume more electrical power followed by increasing ethanol recovery until after 85% ethanol recovery, the overall electrical efficiency then obviously decreases.

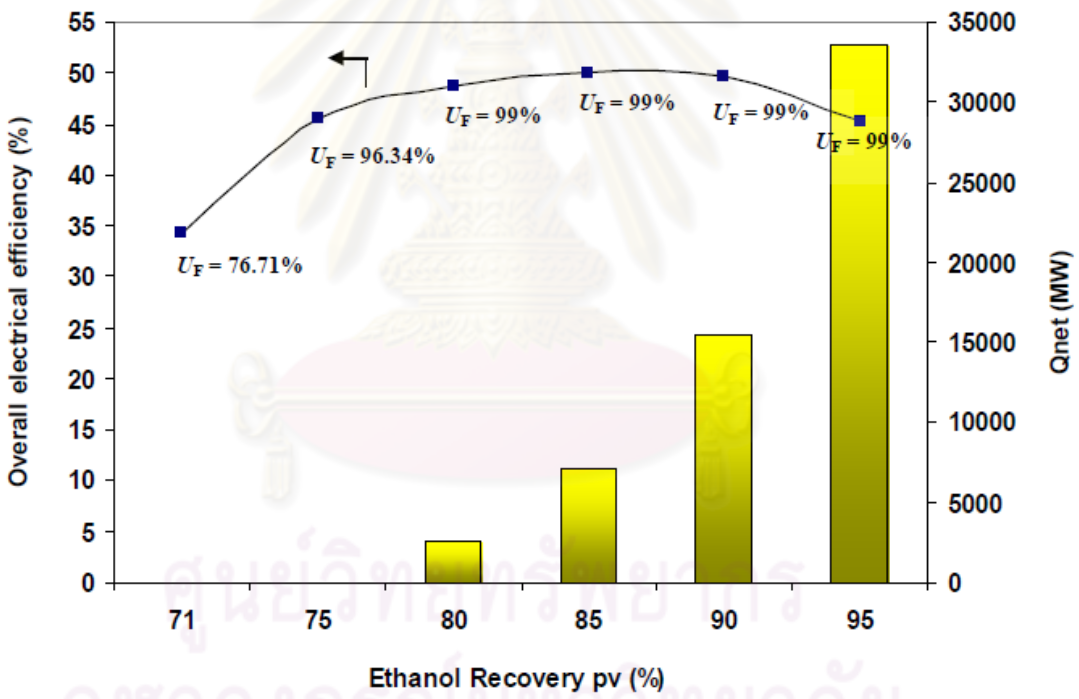

Figure 5.14 Effect of ethanol recovery on the overall electrical efficiency and the net energy (Q_{net}) using hybrid vapor permeation-pervaporation process based on a pervaporation membrane ($\alpha_{E/W}$ = 24).

The separation factor values required for the hydrophilic vapor permeation are presented in Figure 5.15. The values are also compared with the values of separation factor required for hydrophobic pervaporation which provides an equivalent ethanol

recovery at 25 mol% ethanol. At 71% ethanol recovery, the results show that this condition requires only a pervaporation with $\alpha_{E/W}$ = 24.03 which is available in real membrane as shown in Table 5.1 and not necessary to add a vapor permeation expressed as $\alpha_{W/E}$ = 1.12. For a higher ethanol recovery, the obtained separation factor values of hydrophobic pervaporation are too high for its available membrane, while the hydrophilic vapor permeation can be served with real membrane material as in the previous mentioned statement.

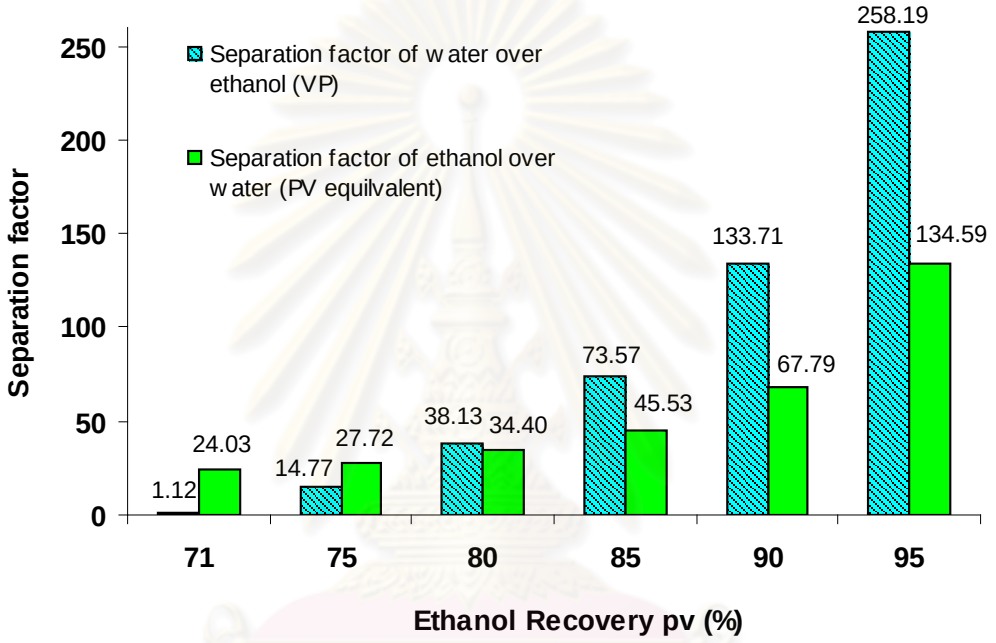

Figure 5.15 A comparison of separation factor between added vapor permeation ($\alpha_{W/E}$) based on pervaporation with $\alpha_{E/W}$ = 24 and pervaporation ($\alpha_{E/W}$).

Finally, the performance of SOFC system integrated with various bioethanol purification processes i.e. conventional distillation column, hybrid vapor permeation-pervaporation and only pervaporation are compared as shown in Figure 5.16. Based on the same ethanol recovery (75%), the results indicate that a use of combined hybrid vapor permeation-pervaporation is regarded as having the best performance for SOFC system which can offer the overall electrical efficiency (45.46%) of about 2 times compared with using a distillation column (22.53%). In case of using only a pervaporation, it can be merely obtained the overall electrical efficiency at 36.46% because its overall system requires more thermal energy than the case of hybrid vapor permeation-pervaporation which has a cooler at vapor

permeation's permeate stream to recover valuable heat from steam to supply the preheater operated at 1023 K as shown in Figure 5.7b). Then its SOFC unit can utilize fuel at high level (96.35%), resulting in the highest overall performance apart from the case of distillation that its SOFC utilizes less fuel to have enough residual fuel for combustion supplying heat to all heat-demanding units especially the reboiler. However, the power density of hybrid vapor permeation-pervaporation is lower than the other two cases because larger SOFC area is required to operate at high fuel utilization.

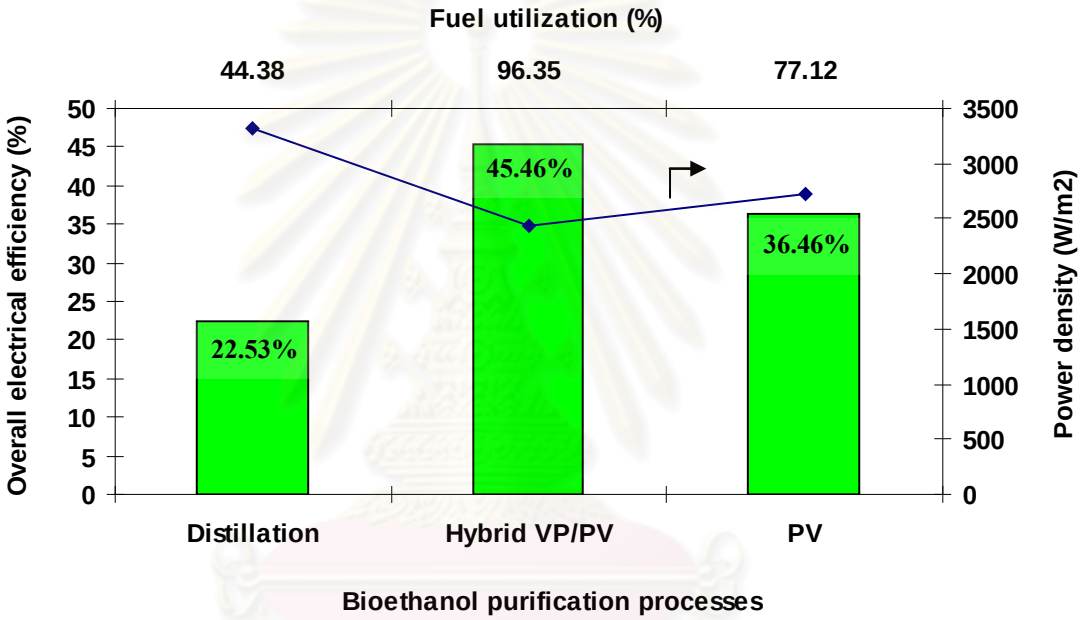

Figure 5. 16 Performance comparison of SOFC system integrated with different bioethanol purification processes based on $Q_{net} = 0$ ($R_{EtOH} = 75\%$, $V = 0.75$V, $T_{SOFC} = 1073$K, $P_p = 0.15$atm).

CHAPTER VI

CONCLUSIONS AND RECOMMENDATIONS

6.1 Conclusions

A pervaporation was applied as a bioethanol purification unit for improving a performance of SOFC system in this research. A selection of appropriate membrane type for pervaporation including hydrophilic and hydrophobic membranes was investigated. A hydrophobic membrane was still considered a suitable membrane type for purifying dilute bioethanol by pervaporation due to low energy consumption, although the availability of this membrane type with high separation factor was one of the concerns particularly when the pervaporation was operated at higher ethanol recovery. Afterwards, a vapor permeation was introduced to install after a hydrophobic pervaporation which was a way to solve the problem of its low separation factor. This proposed purification process can obtain a desired ethanol concentration of 25mol% with higher ethanol recovery. It was found that a hydrophilic type was an appropriate membrane for vapor permeation since it can carry out a higher overall system electrical efficiency than that of the hydrophobic type and also its required membrane separation factor was possibly available in real membrane materials. Although a vacuum pump of hydrophilic vapor permeation consumed high electrical energy at a higher ethanol recovery to remove large amount of steam through a membrane, the total energy requirement was still less than the other case because the required heat is more critical than the required electrical power. Furthermore, there were some conditions at which the system can be operated under energy self-sufficient mode by adjusting proper operating parameters. Based on PTMSP pervaporation regarded as a poorest separation performance among the selected membranes, it can offer the overall electrical efficiency of about 2.4 times when installing an extra vapor permeation unit compared to the case of using a pervaporation alone. Thereafter, ZSM-5/α-Al_2O_3 pervaporation membrane having the highest separation factor ($\alpha_{E/W}$ = 24) among all selected membranes was chosen for the hybrid vapor permeation-pervaporation process. From the system study, it was found that the obtained values

for separation factor of hydrophilic vapor permeation at high ethanol recovery ranges (85-95%) is higher than the separation factor values of hydrophobic pervaporation but these values are still unavailable in real membrane. Moreover, there still remain some useful thermal energy in the SOFC system when using the membrane (ZSM-5/α-Al_2O_3 with $\alpha_{E/W}$ = 24) for pervaporation in the proposed purification process operated at higher ethanol recovery. Finally, the performance of SOFC system integrated with the proposed purification process using this membrane was compared to those of the system using high-energy distillation column to clearly show its efficiency improvement. As a result of the base case study, the overall electrical efficiency received from the proposed purification process (45.46%) can offer about 2 times of the case using a distillation column (22.53%). Particularly at the same ethanol recovery (75%), the hybrid vapor permeation-pervaporation can offer the overall electrical efficiency more than using only a hydrophobic pervaporation (36.46%), indicating that the new proposed purification process in this research has been regarded as the best alternative.

6.2 Recommendations

6.2.1 In the present study, the bioethanol-fuelled SOFC system was investigated using simplified mathematical modeling to demonstrate its feasible performance improvement with the proposed membrane separation processes. It is recommended to develop more sophisticated mathematical models in order to represent more realistic results. The effects of various important operating parameters (e.g. temperature, feed composition and permeate condition) should be investigated to find optimum operating condition and design.

6.2.2 Since a membrane separation unit is usually costly, the economic analysis should be further investigated to evaluate whether the SOFC system integrated with hybrid vapor permeation-pervaporation process can offer some worthwhile benefit with agreeable investment expenditure.

6.2.3 The final case of using hydrophobic pervaporation having $\alpha_{E/W}$ = 24 incorperated with the SOFC system still shows some available heat emitted to environment. Accordingly, it is recommended that excess heat should be recovered by adding combined heat and power (CHP) cogeneration units i.e. turbine, recuperator to increase the efficiency of SOFC system.

REFERENCES

Amphlett, C., Evans, M.J., Jones, R.A., Mann, R.F., and Wier, R.D., Hydrogen production by the catalytic steam reforming of methanol. Part 1. The thermodynamics. Canadian Journal of Engineering 59 (1981): 720.

Arteaga-Perez, L.E., Casas, Y., Peralta, L.M., Kafarov, V., Dewulf, J., and Giunta, P., An auto-sustainable solid oxide fuel cell system fueled by bio-ethanol Process simulation and heat exchanger network synthesis. Chemical Engineering Journal 150 (2009): 242-251.

Chan, S.H., Khor, K.A., and Xia, Z.T., A complete polarization model of a solid oxide fuel cell and its sensitivity to the change of cell component thickness. Journal of Power Sources 93 (2001): 130-140.

Chang, J.H., Yoo, J.K., Ahn, S.H., Lee, K.H., and Ko, S.M., Simulation of pervaporation process for ethanol dehydration by using pilot test results. Korean Journal of Chemical Engineering 15 (1998): 28-36.

Choedkiatsakul, I., et al., Performance improvement of bioethanol-fuelled solid oxide fuel cell system by using pervaporation. International Journal of Hydrogen Energy 36 (2011): 5067-5075.

Claes, S., et al., High flux composite PTMSP-silica nanohybrid membranes for the pervaporation of ethanol/water mixtures. Journal of Membrane Science 351 (2010): 160-167.

Comas, J., Marino, F., Laborde, M., and Amadeo, N., Bio-ethanol steam reforming onNi/Al2O3 catalyst. Chemical Engineering Journal 98 (2004): 61-68.

Dayton, D.C., Fuel cell integration–A study of the impacts of gas quality and impurities. Milestone Completion Report, 2001, pp. 14.

Douvartzides, S.L., Coutelieris, F.A., and Tsiakaras, P.E., On the systematic optimization of ethanol fed SOFC-based electricity generating systems in terms of energy and exergy. Journal of Power Sources 114 (2003): 203-212.

Feng, X., and Huang, R.Y.M., Liquid Separation by Membrane Pervaporation: A Review. Industrial & Engineering Chemistry Research 36 (1997): 1048-1066.

Fergus, J. W., Electrolytes for solid oxide fuel cells. Journal of Power Sources 162 (2006): 30-40.

Hayashi, Y., Yuzaki, S., Kawanishi, T., Shimizu, N., and Furukawa, T., An efficient ethanol concentration process by vapor permeation through a symmetric polyimide membrane. Journal of Membrane Science 177 (2000): 233-239.

Huang, H.J., Ramaswamy, S., Tschirner, U.W., and Ramarao, B.V., A review of separation technologies in current and future biorefineries. Separation and Purification Technology 62 (2008): 1-21.

Huang, Y., Ly, J., Nguyen, D., and Baker, R.W., Ethanol dehydration using hydrophobic and hydrophilic polymer membranes. Industrial & Engineering Chemistry Research 49 (2010): 12067-12073.

Huang, Y., Zhang, P., Fu, J., Zhou, Y., Huang, X., and Tang, X., Pervaporation of ethanol aqueous solution by polydimethylsiloxane/polyphosphazene nanotube nanocomposite membranes. Journal of Membrane Science 339 (2009): 85-92.

Ito, A., Feng, Y., and Sasaki, H., Temperature drop of feed liquid during pervaporation. Journal of Membrane Science 133 (1997): 95-102.

Jamsak, W., et al., Design of a thermally integrated bioethanol-fueled solid oxide fuel cell system integrated with a distillation column. Journal of Power Sources 187 (2009): 190-203.

Jamsak, W., et al., Thermodynamic assessment of solid oxide fuel cell system integrated with bioethanol purification unit. Journal of Power Sources 174 (2007): 191-198.

Kakac, S., Pramuanjaroenkij, A., and Zhou, X.Y., A review of numerical modeling of solid oxide fuel cells. International Journal of Hydrogen Energy 32 (2007): 761 – 786.

Kaneko, T., Brouwer, J., and Samuelsen, G.S., Power and temperature control of fluctuating biomass gas fueled solid oxide fuel cell and micro gas turbine hybrid system. Journal of Power Sources 160 (2006): 316-325.

Ku, B., and Zhang, Y., Status and prospects of intermediate temperature solid oxide fuel cells. Journal of University of Science and Technology Beijing 15 (2008): 84.

Kujawski, W., Application of Pervaporation and Vapor Permeation in Environment Protection. Polish Journal of Environmental Studies 9 (2000): 13-26.

Kumar, S., Singh, N., and Prasad, R., Anhydrous ethanol: A renewable source of energy. Renewable and Sustainable Energy Reviews 14 (2010): 1830-1844.

Lin, X., Chen, X., Kita, H., and Okamoto, K., Synthesis of Silicalite tubular membranes by *In Situ* Crystallization. AlChE Journal 49, 1 (2003): 237-247.

Minh, N.Q., Ceramic Fuel Cells. Journal of the American Ceramic Society 76 (1993): 563-588.

Mulder, M., Basic principles of membrane technology. Amsterdam: Kluwer Academic Publishers 1996.

Naidja, A., Krishna, C.R., Butcher, T., and Mahajan, D., Cool flame partial oxidation and its role in combustion and reforming of fuels for fuel cell systems. Progress in Energy and Combustion Science 29 (2003): 155-191.

Ni, M., Leung, D.Y.C., and Leung, M.K.H., A review on reforming bio-ethanol for hydrogen production. International Journal of Hydrogen Energy 32 (2007): 3238-3247.

Nomura, M., Bin, T., and Nakao, S.I., Selective ethanol extraction from fermentation broth using a silicalite membrane. Separation and Purification Technology 27 (2002):59-66.

Petruzzi, L., Cocchi, S., and Fineschi, F., A global thermo-electrochemical model for SOFC systems design and engineering. Journal of Power Sources 118 (2003): 96-107.

Piroonlerkgul, P., Assabumrungrat, S., Laosiripojana, N., and Adesina, A.A., Selection of appropriate fuel processor for biogas-fuelled SOFC system. Chemical Engineering Journal 140 (2008): 341-351.

Rabenstein, G., and Hacker, V., Hydrogen for fuel cells from ethanol by steam-reforming, partial-oxidation and combined auto-thermal reforming: A thermodynamic analysis. Journal of Power Sources 185 (2008): 1293–1304.

Smith, R., Chemical Process Design and Integration. 2nd Edition, John Wiley & Sons, Ltd., 2005, pp. 199.

Soni, V., Abildskov, J., Jonsson, G., and Gani, R., A general model for membrane-based separation processes. Computers and Chemical Engineering 33 (2009): 644-659.

Tao, G., Armstrong, T., and Virkar, A., Intermediate temperature solid oxide fuel cell (IT-SOFC) research and development activities at MSRI. In: Nineteenth annual ACERC&ICES conference, Utah, 2005.

Vane, L .M., A r eview of pe rvaporation f or pr oduct r ecovery from bi omass fermentation proc esses. Journal of Chemical T echnology a nd B iotechnology 80 (2005): 603-629.

Vane, L.M., Namboodiri, V.V., and Boven, T.C., Hydrophobic zeolite-silicone rubber mixed matrix membranes f or e thanol-water sep aration: E ffect of zeol ite and silicone c omponent s election on pe rvaporation pe rformance. Journal of Membrane Science 308 (2008): 230-241.

Vourliotakis, G., S kevis, G., and F ounti, M.A., Detailed kinetic m odeling of non - catalytic e thanol re forming for S OFC a pplications. International journal of hydrogen energy 34 (2009): 7626-7637.

Wijmans, J.G., and Baker, R.W., The solution-diffusion model: A review. Journal of Membrane Science 107 (1995): 1-21.

Zhang, L., and Yang, W., Direct ammonia solid oxide fuel cell based on thin proton-conducting electrolyte. Journal of Power Sources 179 (2008): 92-95.

Zhao, F., and Virkar, A.V., Dependence of polarization in anode-supported solid oxide fuel cells on various cell parameters. Journal of Power Sources 141 (2005): 79-95.

APPENDICES

APPENDIX A

THERMODYNAMIC DATA OF SELECTED COMPONENTS

Table A1 Heat capacities of selected components (C_p)

Components	$C_p = a + bT + cT^2 + dT^3 + eT^4$ [J/mol K]				
	a	$b \times 10^3$	$c \times 10^5$	$d \times 10^8$	$e \times 10^{13}$
Ethanol	27.091	110.55	10.957	-15.046	461.01
Water	33.933	-8.4186	2.9906	-1.7825	36.934
Methane	34.942	-39.957	19.184	35.103	393.21
Carbon monoxide	29.556	-6.5807	2.0130	-1.2227	22.617
Carbon dioxide	27.437	42.315	-1.9555	0.3997	-2.9872
Hydrogen	25.399	20.178	-3.8549	3.1880	-87.585

Table A2 Heat of formation (H_f) and entropy (S^0) of selected components

Components	$H_f = a + bT + cT^2$ [kJ/mol]			S^o [J/mol.K]
	a	$b \times 10^3$	$c \times 10^5$	
Ethanol	-216.961	-69.572	3.1744	282.59
Water	-241.80	0	0	188.72
Methane	-63.425	-43.355	1.7220	186.27
Carbon monoxide	-112.19	8.1182	-8.0425	197.54
Carbon dioxide	-393.42	0.1591	-0.1395	213.69
Hydrogen	0	0	0	130.57

APPENDIX B

THERMODYNAMIC CALCULATIONS

B1. Determining Gibbs energy (G) at any temperature

Calculation by these equations:

$$G = H - TS \quad \text{(B1)}$$

$$dG = dH - d(TS) \quad \text{(B2)}$$

Integrate the above equation and obtain the solution:

$$\int dG = \int dH - \int d(TS) \quad \text{(B3)}$$

$$G_T - G_{STD} = \int_{298}^{T} dH - \int_{298}^{T} d(TS) \quad \text{(B4)}$$

where

$$H_f(T) = H_f^o + \int_{298}^{T} C_p \, dT \quad \text{(B5)}$$

$$S(T) = S^o + \int_{298}^{T} \frac{C_p}{T} dT \quad \text{(B6)}$$

B2. Determining the equilibrium constant (K)

$$G_T = RTlnK \quad \text{(B7)}$$

Rearrange the equation:

$$K = \exp(-\frac{G_T}{RT}) \quad \text{(B8)}$$

APPENDIX C

LIST OF PUBLICATIONS

International Conference

V. Sukwattanajaroon, S. Charojrochkul, W. Kiatkittipong, W. Wiyaratn, A. Soottitantawat, A. Arpornwichanop, N. Laosiripojana and S. Assabumrungrat; "Effect of membrane type on performance of bioethanol-fuelled solid oxide fuel cell system integrated with pervaporation", Regional Symposium on Chemical Engineering (RSCE 2010), Bangkok, November 22-23, 2010 (oral presentation).

National Publication

Vorachatra Sukwattanajaroon, Sumittra Charojrochkul, Worapon Kiatkittipong, Amornchai Arpornwichanop and Suttichai Assabumrungrat, Performance of membrane-assisted solid oxide fuel cell system fuelled by bioethanol, Engineering Journal 15, 2 (2011): 53-66.

VITAE

Mr. Vorachatra Sukwattanajaroon was born in May 4th, 1987 in Bangkok, Thailand. He finished high school from Sarawittaya School, Bangkok in 2005, and received his Bachelor's Degree in Chemical Engineering from the Department of Chemical Engineering, Faculty of Engineering, Chulalongkorn University, Bangkok in 2009. Afterward, he continued studying Master's Degree of Chemical Engineering, Chulalongkorn University since June 2009.